and 0.0025% bromophenol blue) and boiled for 5min. The samples were electrophoresed in 10% SDS-PAGE and the proteins were transferred to nylon membrane, Hybond-P (Amersham Biosciences Corp., Piscataway, NJ, USA). After blocking with 5% skim milk, L1 protein was probed by anti-HPV 16 L1 mouse monoclonal antibody (554171, Becton Dickinson Co. Ltd., San Diego, CA, USA). Horseradish peroxidase conjugated anti-mouse IgG goat antibodies (SC-2031, Santa Cruz Biotechnology, Inc., Santa Cruz, CA, USA) and ECL Western Blotting Detection System (Amersham Biosciences Corp.) were used to detect mouse IgG on the membrane. The fluorescence were detected by Storm Phosphor Imager (Amersham Biosciences Corp.).

*Northern blotting*

Total RNA was isolated by using RNeasy mini kits (Qiagen, Hilden, Germany) according to the manufacturers' instructions. PolyA RNA was isolated by using oligo dT cellulose (micro mRNA purification kit, Amersham Biosciences Corp.) according to the manufacturers' instructions. RNA (10 $\mu$g for total RNA, 2 $\mu$g for polyA RNA) was electrophoresed on 1% agarose gel, and transferred to a nylon membrane (Hybond-XL, Amersham Biosciences Corp.). $^{32}$P-labeled probes were prepared by Rediprime II DNA labelling system (Amersham Biosciences Corp.). The intensities of each band was quantified by Storm Phosphor Imager (Amersham Biosciences Corp.).

*Analysis of mRNA stability*

293T cells transfected with the expression plasmids were incubated for 2 days, and then harvested (0 h), or incubated with ActinomycinD (5$\mu$g/ml; Sigma-Aldrich, St. Louis, MO, USA) for a further 0.5, 2, and 8 h before harvesting. PolyA RNA was extracted, and firefly luciferase-mRNA and renilla luciferase-mRNA were detected by the Northern blotting as described above.

## Results

*Expression of L1 from the codon modified mutant*

We confirmed previous findings that HPV16 L1 encodes an RNA element negatively regulates L1 expression [18]. A codon-modified HPV16 L1 mutant was newly constructed in a way similar to that in the previous report [18]. As described in Materials and Methods, the majority of codons were changed into those used most frequently in human mRNAs without affecting the encoded protein sequence. Our codon modification inactivated the inhibitory RNA elements present in the HPV16 L1 coding region (Figs. 1A and 1B).

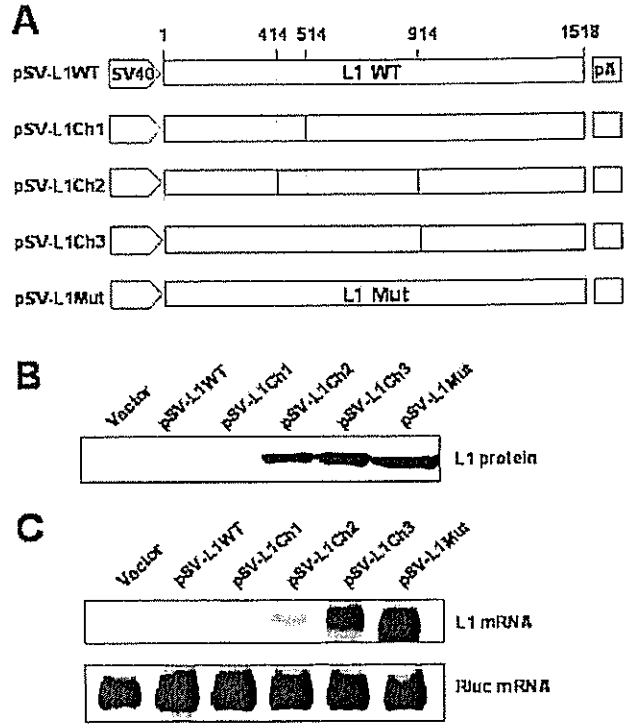


*Fig. 1.* Expression of HPV16 L1 from SV40 promoter in 293T cells (A) Schematic representation of the chimera L1 genes composed of the authentic and a codon-modified L1 genes, L1 WT: authentic L1 gene; L1 Mut: codon-modified L1 gene; SV40: SV40 early promoter; pA: SV40 late poly A signal. (B) Western blotting to detect L1, 293T cells were transfected with the expression plasmid and 48h later cell lysate was analyzed by Western blotting with anti-HPV16L1 mouse monoclonal antibody. (C) Northern blotting to detect L1-mRNA, 293T cells were transfected with the mixture of an expression plasmid for L1 and pEF1a-renilla, an expression plasmid for renilla luciferase. Total RNA was extracted at 48h after the transfection. PolyA RNA was purified by oligo-dT column chromatography and analyzed by Northern blotting with radio-labeled mixed probes hybridizing with the entire coding region of authentic L1 and codon-modified L1 genes (indicated as L1 mRNA). Then the membrane was re-probed with a radio-labeled probe hybridizing with renilla luciferase sequences (Rluc mRNA).

HPV16 L1 was not produced in 293T cells transfected with pSV-L1WT, an SV40 early promoter-driven expression plasmid for the wild-type L1 gene, but was efficiently produced in those transfected with pSV-L1Mut, the one for the codon-modified gene, which is consistent with the previous findings that L1 was efficiently produced in 293T cells transfected with CMV promoter-driven expression plasmid for similar codon-modified L1 gene [18].

The major inhibitory cis-element was located within the first 514 nucleotides as previously indicated by analyses of expressions from fusion genes of HPV16 L1 and EIAV p55gag [16]. Expression plasmids for chimeric L1 genes were produced by replacement of regions from nt1 to nt514, from nt414 to nt914, and from nt914 to nt1518 (A of the first ATG

of the L1-coding region was numbered as nt1) of pSV-L1Mut with the corresponding regions of the authentic L1 gene to produce pSV-L1Ch1, pSV-L1Ch2, and pSV-L1Ch3, respectively (Fig. 1A). L1 was not produced in 293T cells transfected with pSV-L1Ch1 (Fig. 1B). L1 was produced from pSV-L1Ch2 less efficiently than from pSV-L1Ch3 (Fig. 1B). The level of L1 produced from pSV-L1Ch3 was comparable to that from pSV-L1Mut (Fig. 1B).

The L1 levels were parallel with the levels of L1-mRNA as previously reported [16]. PolyA RNA was obtained from 293T cells transfected with each of the L1-expression plasmid. Level of L1-mRNA was examined by Northern blotting (Fig. 1C). L1-mRNAs from pSV-L1WT and from pSV-L1Ch1 were not detected. L1-mRNA from pSV-L1Ch2 was easily detected and those from pSV-L1Ch3 and from pSV-L1Mut were abundant. For monitoring transfection efficiency, 293T cells were co-transfected with an expression plasmid for renilla luciferase, and the level of the mRNA (Rluc) was examined by re-probing the membrane used for detection of L1-mRNA (Fig. 1C). The data indicate that as previously reported [16], the major inhibitory RNA element, which reduces the steady-state level of mRNA, is present within the first 514 nucleotides. In an attempt to elucidate how the element works, we subsequently used the DNA fragment encoding the cis-element to examine its effect on the mRNA from heterologous genes in 293T cells.

*Steady-state level of heterologous mRNA having the major inhibitory element*

The steady-state level of firefly luciferase (Fluc)-mRNA having the major inhibitory RNA element near the 5′ end was lower than that of the authentic Fluc-mRNA. The L1 DNA fragment containing the region encoding the major inhibitory element (from nt4 to nt513 of the L1 coding region, designated as the inhibitory region: IR) was inserted into Fluc at its various sites. The resultant fusion genes were ligated with the SV40 early promoter to produce a series of expression plasmids (Fig. 2A). p5′UTR-IRLuc and p3′UTR-IRLuc had IR in 5′ UTR and 3′ UTR, respectively. p3-IRLuc has IR at nt3 (the A at the first ATG of the Fluc-coding region was numbered as nt1 in these fusion genes) in frame. The other expression plasmids were named similarly. 293T cells were transfected with each expression plasmid and polyA RNA was obtained from the cells at 48 h after the transfection. The steady-state level of the fusion gene-mRNA was detected by Northern blotting (Fig. 2B). The mRNAs transcribed from p5′UTR-IRLuc, p3-IRLuc, p171-IRLuc, and p582-IRLuc were not detected (Fig. 2B). The longer the distance between the 5′ end of Fluc gene and IR was, the higher the level of the mRNA was. The level of p1650-IRLuc-mRNA was comparable to

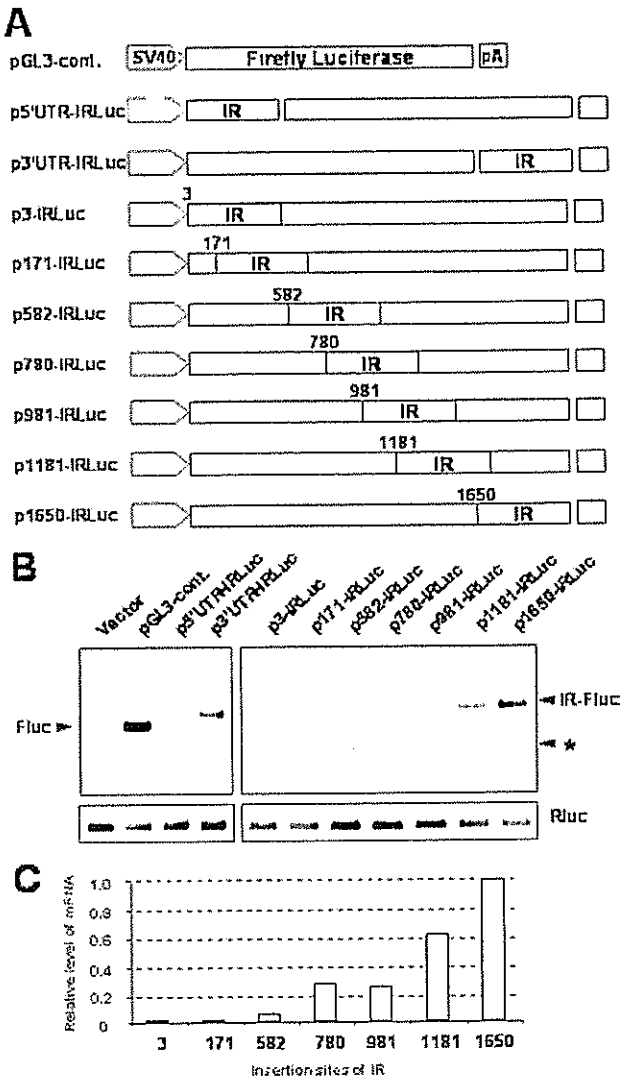


*Fig. 2.* Steady-state level of firefly luciferase-mRNA having the major inhibitory element (A) Schematic representation of the fusion genes composed of firefly luciferase gene and the L1-fragment encoding the major inhibitory element. IR: DNA fragment of HPV16 L1 from nt4 to nt513. A at the first ATG of firefly luciferase gene is numbered as 1. (B) Northern blotting to detect firefly luciferase-mRNA, 293T cells were transfected with the mixture of one of the expression plasmids for firefly lusiferase and pEF1a-renilla. Total RNA was extracted at 48h after the transfection. PolyA RNA was purified by oligo-dT column chromatography and analyzed by Northern blotting with a radio-labeled probe hybridizing with the entire coding region of firefly luciferase gene (indicated as Fluc). Then the membrane was re-probed with a radio-labeled probe hybridizing with the entire coding region of renilla luciferase gene (Rluc). The minor transcript from the cryptic promoter within the firefly luciferase coding region is indicated by an asterisk. (C) Relative levels of mRNA of the fusion genes. The intensity of the band obtained by the above Northern blotting was measured by Storm Phosphor Imager (Amersham Biosciences Corp.) and normalized against that of the renilla luciferase-mRNA.

that of pGL3-control-mRNA, the negative element-free authentic mRNA (Fig. 2B).

A minor transcript, indicated by an asterisk in Fig. 2B, was detected by Northern blotting in the polyA RNA samples extracted from 293T cells transfected with pGL3-control, p5′UTRIRLuc, p3-IRLuc, p171-IRLuc, and p582-IRLuc. A rapid amplification of cDNA ends (5′-RACE) analysis of the transcript from p3-IRLuc revealed that 5′-end of the most of the transcripts was nt 644 of the FLuc ORF, indicating that a cryptic promoter was present within the FLuc ORF. The data indicate that IR existing upstream of the cryptic promoter did not affect the steady-state levels of the polyA RNA transcribed from the cryptic promoter. When the IR was present downstream of nt 644, as in p3′UTRLuc, p780-IRLuc, p981-IRLuc, p1181-IRLuc and p1650-IRLuc, the steady-state levels of the minor polyA RNA transcribed from the cryptic promoter became undetectable. The effect of IR on the polyA RNA from the cryptic promoter was similar to that on the polyA RNA from SV40 promoter.

Insertion of IR into the EGFP gene (Fig. 3) and $\beta$-gal gene (Fig. 4) resulted in reduced steady-state mRNA levels of the fusion genes. Similarly, the efficiency of the mRNA-reduction depended on the relative position of IR in the fusion gene. The data indicate that the putative major inhibitory element down-regulates the steady-state level of heterologous mRNA. The efficient inhibition is obtained when the element is placed near the 5′ end of the fusion gene-mRNA.

Previously it was reported that the insertion of the first 367 nucleotides of the L1 gene into the 5′ ends of EIAV p55gag gene and CAT gene efficiently reduced the mRNA steady-state levels and that the insertion of the region into the 3′ end of EIAVp55 gene less efficiently reduced the mRNA steady-state level [16]. Together with the previous findings, the data in this study indicate that IR near 5′ end of a gene induces strong reduction of the mRNA in general.

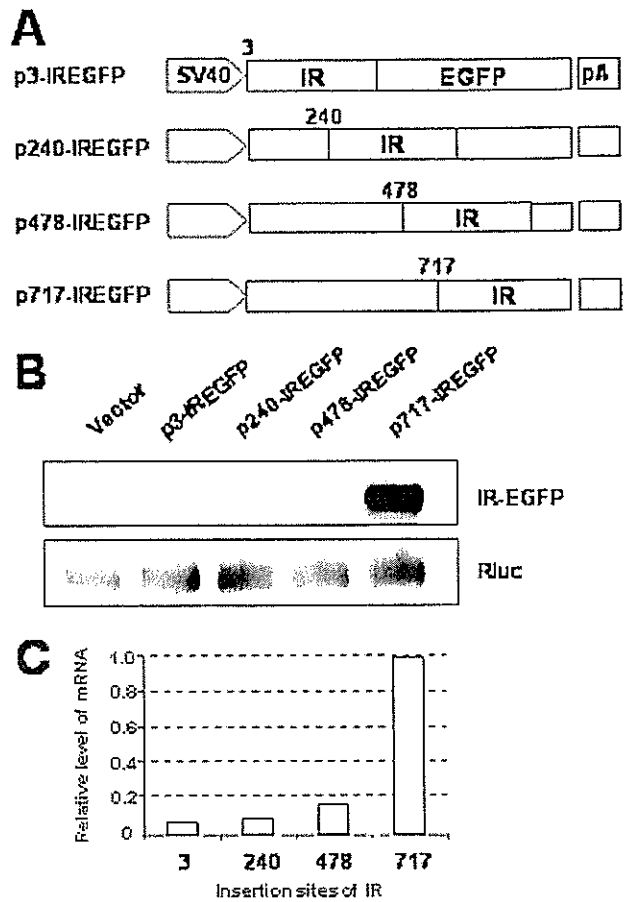


*Fig. 3.* Steady-state level of EGFP-mRNA having the major inhibitory RNA element, (A) Schematic representation of the fusion genes composed of EGFP gene and the L1-fragment encoding the major inhibitory element. IR: DNA fragment of HPV16 L1 from nt4 to nt513. A at the first ATG of EGFP gene is numbered as 1. (B) Northern blotting to detect EGFP-mRNA, 293T cells were transfected with the mixture of one of the expression plasmids for EGFP with IR and pEF1a-renilla. Total RNA was extracted at 48h after the transfection. PolyA RNA was purified by oligo-dT column chromatography and analyzed by Northern blotting with a radio-labeled probe hybridizing with the entire coding region of EGFP gene (indicated as EGFP). Then the membrane was re-probed with a radio-labeled probe hybridizing with renilla luciferase sequences (Rluc). (C) Relative levels of mRNA of the fusion genes. The intensity of the band obtained by the above Northern blotting was measured by Storm Phosphor Imager (Amersham Biosciences Corp.) and normalized against that of the renilla luciferase-mRNA.

*Stability of the mRNA having the major inhibitory element*

The reduced steady-state level of the mRNA having the RNA derived from IR (IR-RNA) was probably not due to the quick degradation of the mRNA. Since the level of mRNA from p582-IRLuc was much lower than that from p1650-IRLuc (Fig. 2B), we examined whether the half-life of p582-IRLuc-mRNA was shorter than that of p1650-IRLuc-mRNA. 293T cells were transfected with p582-IRLuc, p1650-IRLuc, or pGL3-control. Two days later Actinomycin D (5$\mu$g/ml) was added to the culture medium of the cells to inhibit de novo RNA synthesis. Total RNA was extracted at 0, 0.5, 2, and 8h after the addition of Actinomycin D. PolyA-RNA was purified by oligo-dT column chromatography and electrophoresed on agarose-gel. The Fluc-fusion gene-mRNA was analyzed by Northern blotting with radio-labeled probe specific to Fluc (Fig. 5A). The steady-state level of the mRNA from p582-IRLuc was approximately 1/17 of those from p1650-IRLuc and pGL3-control (Fig. 2 and Fig. 6A, time 0). After the interruption of RNA synthesis by Actinomycin D, the levels of the mRNAs from p582-IRLuc, p1650-IRLuc, and pGL3-control lowered similarly (Fig. 5B), indicating that the three mRNA species were degraded with a

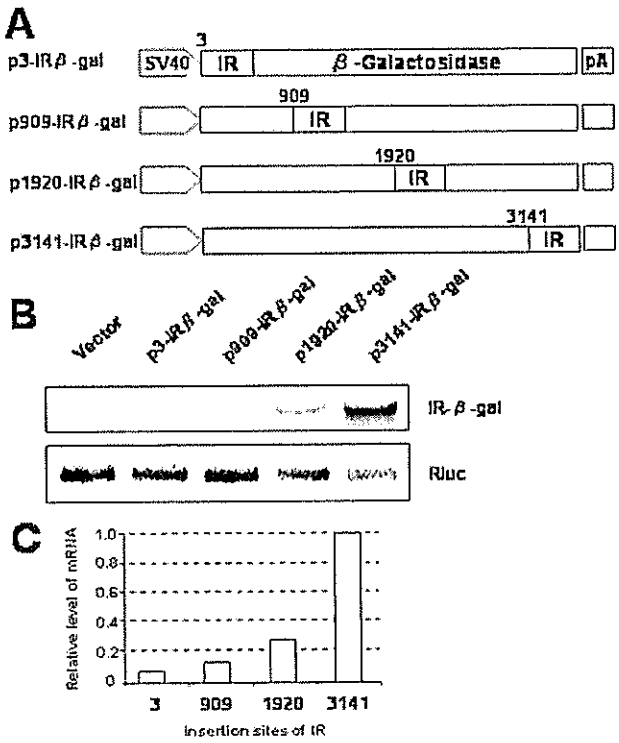


*Fig. 4.* Steady-state level of β-galactosidase-mRNA having the major inhibitory RNA element, (A) Schematic representation of the fusion genes composed of β-galactosidase gene and the L1-fragment encoding the major inhibitory element. IR: DNA fragment of HPV16 L1 from nt4 to nt513. A at the first ATG of β-galactosidase gene is numbered as 1. (B) Northern blotting to detect β-galactosidase-mRNA, 293T cells were transfected with the mixture of one of the expression plasmids for β-galactosidase with IR and pEF1a-renilla. Total RNA was extracted at 48h after the transfection. PolyA RNA was purified by oligo-dT column chromatography and analyzed by Northern blotting with a radio-labeled probe hybridizing with the entire coding region of β-galactosidase gene (indicated as β-gal). Then the membrane was re-probed with a radio-labeled probe hybridizing with renilla luciferase sequences (Rluc). (C) Relative levels of mRNA of the fusion genes. The intensity of the band obtained by the above Northern blotting was measured by Storm Phosphor Imager Amersham Biosciences Corp.) and normalized against that of the renilla luciferase-mRNA.

similar efficiency. Thus, the major inhibitory element near the 5′ end of the mRNA does not enhance degradation of the matured mRNA.

It was shown previously that the half-life of mRNA transcribed from CAT gene having the first 129 nucleotides of the L1 gene, the minimum region that reduced the mRNA steady-state level, was slightly shorter than that from CAT gene having the codon-modified corresponding region [16]. However, the shortened half-life did not fully account for the reduced steady-state level of the mRNA [16].

*Removal of the major inhibitory element from transcript by splicing*

Down-regulation of the steady-state mRNA level by IR placed at the 5′ end of Fluc gene was abolished by removal of the IR-RNA by splicing. The SV40 splicing donor (SD) and acceptor (SA) signals were inserted at the 5′ and 3′ sides of IR in p5′UTR-IRLuc and p3′UTR-IRLuc, respectively, to produce p5′UTR-IRspl and p3′UTR-IRspl (Fig. 6A). For comparison, the consensus sequences of SD and SA were mutated to produce mSD and mSA, respectively, and inserted into the plasmids (Fig. 6A). PolyA RNA prepared from 293T cells transfected with each of the plasmids was analyzed by Northern blotting with radio-labeled probe specific to Fluc (Fig. 6B). The spliced form of mRNA from p5′UTR-IRspl was readily detected, although the unspliced form of mRNA from p5′UTR-IRmspl was not. A very low level of the spliced form of mRNA from p5′UTR-IRmspl was detected, indicating that a low level of splicing occurred with the mutated donor and the mutated acceptor signals. Both spliced and unspliced forms of mRNA from p3′UTR-IR-spl and the unspliced mRNA from p3′UTR-IRmspl were detected. The data suggest that the transcription of the gene having IR proceeds normally and that IR-RNA in the transcript mediates the reduction of the steady-state level of mRNA after the splicing step in the mRNA processing.

The minor mRNA (indicated by the asterisk) transcribed from the cryptic promoter was detected in the samples from p5′UTR-IRspl and p5′UTR-IRmspl, but was not detected in the samples from p3′UTR-IRspl and p3′UTR-IRmspl. Recently, Zhao *et al.* [25] reported that the RNA element in the L1 coding region suppressed function of the splicing acceptor signal existing upstream of the HPV16 L1 coding region in the context of the HPV16 late genes. The RNA element may affect the splicing with the signals located near the element.

*Steady-state level of RNA polymerase-I-transcribed RNA having the major inhibitory element*

The inhibitory effect of IR-RNA was not observed when transcription was directed by the HrD promoter that uses RNA polymerase-I for RNA synthesis. Since the reduced steady-state level of mRNA having IR-RNA was not ascribed to the shorter half-life of the matured mRNA, we speculated that the transcript having IR-RNA might degrade in the course of mRNA maturation. RNA synthesized by RNA polymerase-I, which is used to produce ribosomal RNA, is not processed as RNA synthesized by RNA polymerase-II. The SV40 early promoter in pGL3-control, p5′UTR-IRLuc and p3′UTR-IRLuc was replaced by the HrD promoter to produce pHrD-Luc, pHrD-5′IRLuc and pHrD-3′IRLuc, respectively (Fig. 7A). 293T cells were

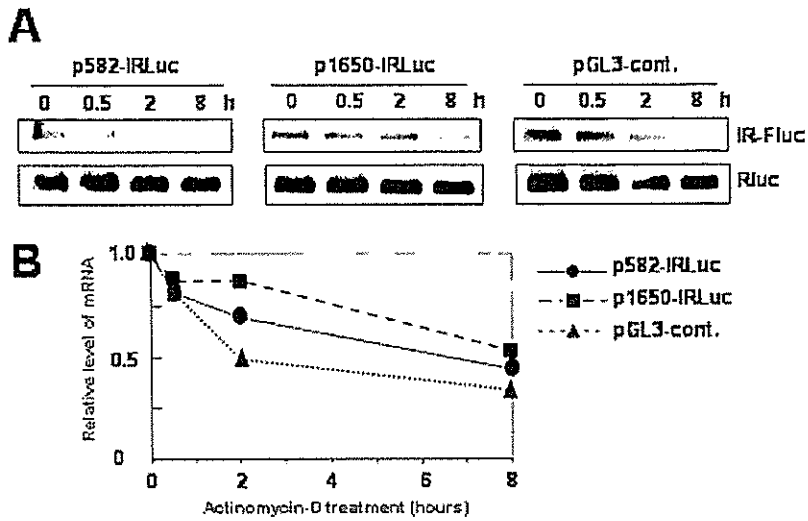


*Fig. 5.* Stability of the mRNA having the major inhibitory element (A) Northern blotting to detect firefly luciferase-mRNA 293T cells were transfected with p582-IRLuc, p1650-IRLuc, or pGL3-control (see Fig. 2). Two days later Actinomycin D (5$\mu$g/ml) was added to the culture medium. Total RNA was extreacted before the addition of the drug (for sample 0) and 0.5, 2, and 8 h after the addition of the drug. PolyA RNA was purified by oligo-dT column chromatography and analyzed by Northern blotting with a radio-labeled probe hybridizing with firefly luciferase sequences (indicated as Fluc). Then the membrane was re-probed with a radio-labeled probe hybridizing with the entire coding region of renilla luciferase gene (Rluc). (B) Relative degradation rate of the mRNA with and without the major inhibitory element, The intensity of the band obtained by the above Northern blotting was measured by Storm Phosphor Imager (Amersham Biosciences Corp.), normalized against that of the renilla luciferase-mRNA, and plotted as the relative level against the level of sample obtained at 0 h.

transfected with each of these expression plasmids and total RNA was extracted at 48h after the transfection. The RNA hybridizing with radio-labeled probes specific to Fluc was analyzed by Northern blotting (Fig. 7B). The steady state level of Fluc-RNA from p5′UTR-IRLuc was virtually undetectable. However, the steady state level of Fluc-RNA from pHrD-5′IRLuc was comparable to that from pHrD-3′IRLuc. The data strongly suggest that the major inhibitory element works in association with the cellular machinery for mRNA maturation.

## Discussion

In this study we analyzed the RNA degradation mediated by the HPV16 L1 major inhibitory cis-element, using the Fluc-mRNA having the element as a model RNA. The steady-state level of the fusion-Fluc-mRNA was down-regulated by the element with the efficiency depending on the distance from the 5′ end of the mRNA to the element, suggesting that the probable interactions of the inhibitory element with the 5′ end mRNA is important. It is possible that the cap structure may be involved in the RNA degradation. The level of the Fluc-mRNA having the element at 582 nucleotides from the 5′ end was approximately 1/17 that of the Fluc-mRNA having the element at the 3′ end, but both mRNAs had a similar half-life. This indicates that once matured, the mRNA with the element is as stable as the one without, and that the decay occurs before the maturation of mRNA. The Fluc-mRNA having the element near the 5′ end was undetectable, but removal of the element by splicing resulted in emergence of the easily detectable mRNA lacking the element. Involvement of the cellular machinery for mRNA-maturation was further suggested from the fact that the stable RNA with the cis-element was synthesized by RNA polymerase-I, which is known to produce unprocessed RNA. Thus, the results of this study are likely to indicate that the inhibitory cis-element-mediated RNA decay takes place after splicing and before the completion of mRNA maturation, probably using the cellular machinery for mRNA processing.

Leder *et al.* [18] examined IRES-mediated expression of GFP from bicistronic mRNA having the L1 gene placed upstream of the IRES by using a CMV promoter-driven expression plasmid. The Level of GFP from the fusion gene having the codon-modified L1 gene was 5 times higher than that from the fusion gene having the authentic L1 gene, although the level of L1 from the codon-modified L1 gene was 1,000 times higher than that from the authentic L1 gene. They concluded that adaptation for codon usage accounts for the vast majority of the improvement in protein expression, whereas transcriptional events contribute only to a minor degree. We cannot discuss the reason for the discrepancy between our and Leder *et al.*'s conclusions because Leder *et al.* did not analyze the levels of the mRNA. The results in this study

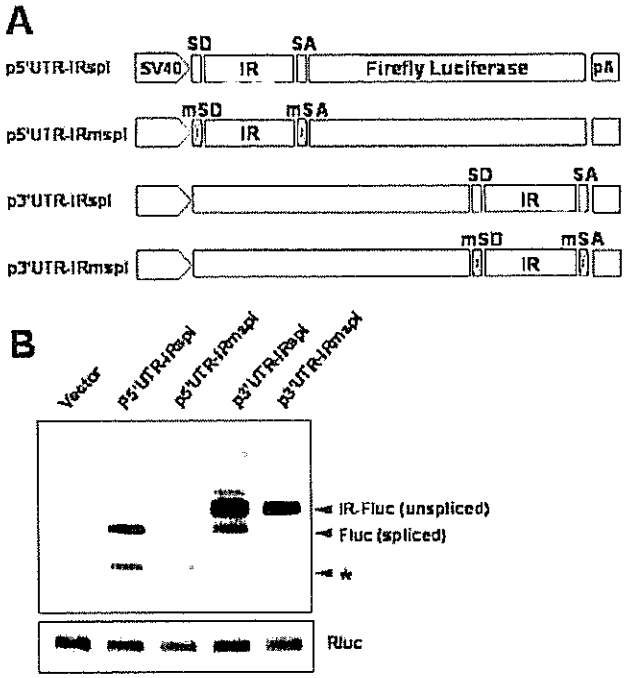


*Fig. 6.* Steady-state level of firefly luciferase-mRNA whose major inhibitory RNA element was removed by splicing, (A) Schematic representation of the firefly genes that have IR sandwiched by the SV40 splicing signals. IR: DNA fragment of HPV16 L1 from nt4 to nt513. SD: SV40 splicing donor signal; SA: SV40 splicing acceptor signal; mSD: inactivated SD by nucleotide substitutions; mSA: inactivated SA by nucleotide substitutions, (B) Northern blotting to detect firefly luciferase-mRNA, 293T cells were transfected with the mixture of one of the expression plasmids for firefly lusiferase and pEF1a-renilla. Total RNA was extracted at 48h after the transfection. PolyA RNA was purified by oligo-dT column chromatography and analyzed by Northern blotting with a radio-labeled probe hybridizing the entire coding region of firefly luciferase gene (indicated as Fluc). Then the membrane was re-probed with a radio-labeled probe hybridizing with the entire coding region of renilla luciferase gene (Rluc). The minor transcript from the cryptic promoter within the firefly luciferase coding region is indicated by an asterisk.

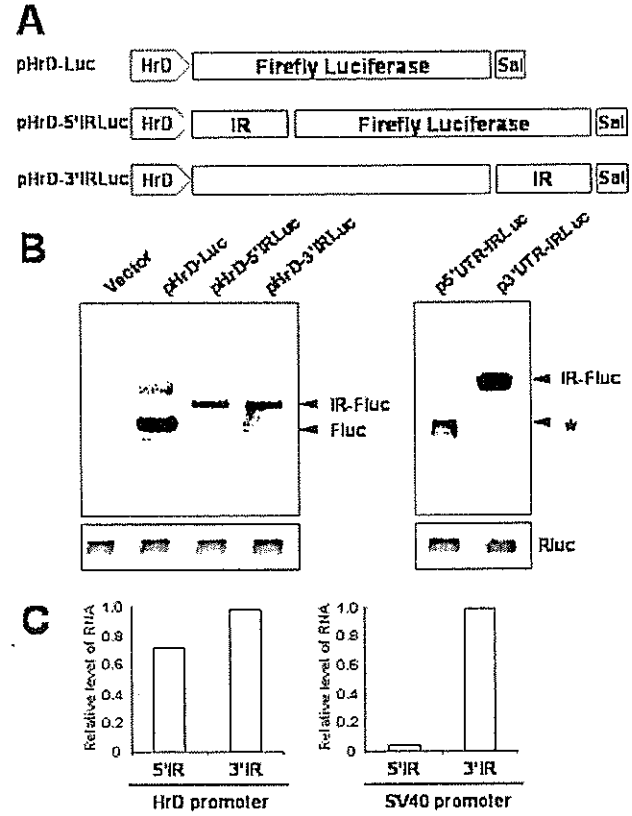


*Fig. 7.* Steady-state level of RNA polymarase-I synthesized-firefly luciferase-RNA having the major inhibitory element, (A) Schematic representation of the fusion genes composed of firefly luciferase gene and the L1-fragment encoding the major inhibitory element. HrD: a promoter directing RNA synthesis by RNA polymerase-I; IR: DNA fragment of HPV16 L1 from nt4 to nt513; Sal: Sal box, the termination signal for RNA synthesis by RNA polymerase-I. (B) Northern blotting to detect firefly luciferase-RNA, 293T cells were transfected with the mixture of one of the expression plasmids for firefly lusiferase and pEF1a-renilla. Total RNA was extracted at 48h after the transfection and analyzed by Northern blotting with a radio-labeled probe hybridizing with the entire coding region of firefly luciferase gene (indicated as Fluc). Then the membrane was re-probed with a radio-labeled probe hybridizing with the entire coding region of renilla luciferase gene (Rluc). The minor transcript from the cryptic promoter within the firefly luciferase coding region is indicated by an asterisk. (C) Relative levels of RNA of the fusion genes. The intensity of the band obtained by the above Northern blotting was measured by Storm Phosphor Imager (Amersham Biosciences Corp.) and normalized against that of the renilla luciferase-mRNA.

totally agree with the previous results presented by Collier *et al.* [16].

The negative regulation may be important for the part of HPV16 life cycle; L1 is expressed only in the upper layers of the epithelium [4]. For the extremely limited L1 expression in the terminally differentiating keratinocytes, HPV probably takes advantage of cellular mechanism for regulation of differentiation-specific gene expression. The negative regulation may be inactivated by cellular factor(s) emerging in the differentiating keratinocytes.

Down-regulation of mRNAs by cis-acting RNA elements in the coding regions have been reported for some cellular mRNAs from genes, such as, *c*-fos [26, 27], c-myc [28], and beta-tubulin [29]. The regulation of these mRNAs is coupled with translation, and the degradation occurs in the cytoplasm. In the case of mRNA for folate receptor type alpha (FR-alpha), the mRNA is degraded in the nucleus by unknown mechanism [30]. Degradation of pre-mRNA in the course of mRNA maturation, as HPV16 L1-mRNA, has been found for mRNAs from genes, such as, alpha 1-acid glycoprotein (AGP) [31], spot 14 [32], class I major histocompatibility complex (MHC) [33], dihydrofolate reductase (DHFR) [34], myeloperoxidase [35],

granulocyte-macrophage colony-stimulating factor (GM-CSF) [36], and peptidylglycine alpha-amidating monooxygenase (PAM) genes [37]. Expression of these genes seems to be regulated very strictly. Molecular details of the post-transcriptional regulation remain unknown.

## Acknowledgments

We thank Dr. Kunito Yoshiike for critical reading of the manuscript. This work was supported by a grant-in-aid from the Ministry of Health, Labour and Welfare for the Third-Term Comprehensive Control Research for Cancer and for the Research on Human Genome and Tissue Engineering.

## References

1. zur Hausen H: Papillomavirus infections – a major cause of human cancers. Biochim Biophys Acta 1288: F55–F78, 1996
2. de Villiers EM, Fauquet C, Broker TR, Bernard HU, zur Hausen H: Classification of papillomaviruses. Virology 324: 17–27, 2004
3. Stoler MH, Broker TR: In situ hybridization detection of human papillomavirus DNAs and messenger RNAs in genital condylomas and a cervical carcinoma. Hum Pathol 17: 1250–1258, 1986
4. Laimins LA: The biology of human papillomaviruses: from warts to cancer. Infect Agents Dis 2: 74–86, 1993
5. O'Connor MJ, Stunkel W, Koh CH, Zimmermann H, Bernard HU: The differentiation-specific factor CDP/Cut represses transcription and replication of human papillomaviruses through a conserved silencing element. J Virol 74: 401–410, 2000
6. Kukimoto I, Kanda T: Displacement of YY1 by differentiation-specific transcription factor hSkn-1a activates the P(670) promoter of human papillomavirus type 16. J Virol 75: 9302–9311, 2001
7. Kennedy IM, Haddow JK, Clements JB: Analysis of human papillomavirus type 16 late mRNA 3′ processing signals in vitro and in vivo. J Virol 64: 1825–1829, 1990
8. Tan W, Schwartz S: The Rev protein of human immunodeficiency virus type 1 counteracts the effect of an AU-rich negative element in the human papillomavirus type 1 late 3′ untranslated region. J Virol 69: 2932–2945, 1995
9. Sokolowski M, Zhao C, Tan W, Schwartz S: AU-rich mRNA instability elements on human papillomavirus type 1 late mRNAs and c-fos mRNAs interact with the same cellular factors. Oncogene 15: 2303–2319, 1997
10. Sokolowski M, Furneaux H, Schwartz S, The inhibitory activity of the AU-rich RNA element in the human papillomavirus type I late 3′ untranslated region correlates with its affinity for the elav-like HuR protein. J Virol 73: 1080–1091, 1999
11. Dietrich-Goetz W, Kennedy IM, Levins B, Stanley MA, Clements JB: A cellular 65-kDa protein recognizes the negative regulatory element of human papillomavirus late mRNA. Proc Natl Acad Sci USA 94: 163–168, 1997
12. Furth PA, Choe WT, Rex JH, Byrne JC, Baker CC: Sequences homologous to 5′ splice sites are required for the inhibitory activity of papillomavirus late 3′ untranslated regions. Mol Cell Biol 14: 5278–5289, 1994
13. Koffa MD, Graham SV, Takagaki Y, Manley JL, Clements JB: The human papillomavirus type 16 negative regulatory RNA element interacts with three proteins that act at different posttranscriptional levels. Proc Natl Acad Sci USA 97: 4677–4682, 2000
14. Kennedy IM, Haddow JK, Clements JB: A negative regulatory element in the human papillomavirus type 16 genome acts at the level of late mRNA stability. J Virol 65: 2093–2097, 1991
15. Sokolowski M, Tan W, Jellne M, Schwartz S: mRNA instability elements in the human papillomavirus type 16 L2 coding region. J Virol 72: 1504–1515, 1998
16. Collier B, Öberg D, Zhao X, Schwartz S: Specific inactivation of inhibitory sequences in the 5′ end of the human papillomavirus type 16 L1 open reading frame results in production of high levels of L1 protein in human epithelial cells. J Virol 76: 2739–2752, 2002
17. Öberg D, Collier B, Zhao X, Schwartz S: Mutational inactivation of two distinct negative RNA elements in the human papillomavirus type 16 L2 coding region induces production of high levels of L2 in human cells. J Virol 77: 11674–11684, 2003
18. Leder C, Kleinschmidt JA, Wiethe C, Müller M: Enhancement of capsid gene expression: preparing the human papillomavirus type 16 major structural gene L1 for DNA vaccination purposes. J Virol 75: 9201–9209, 2001
19. Tan W, Felber BK, Zolotukhin AS, Pavlakis GN, Schwartz S: Efficient expression of the human papillomavirus type 16 L1 protein in epithelial cells by using Rev and the Rev-responsive element of human immunodeficiency virus or the cis-acting transactivation element of simian retrovirus type 1. J Virol 69: 5607–5620, 1995
20. Browne HM, Churcher MJ, Stanley MA, Smith GL, Minson AC: Analysis of the L1 gene product of human papillomavirus type 16 by expression in a vaccinia virus recombinant. J Gen Virol 69: 1263–1273, 1988
21. Heino P, Dillner J, Schwartz S: Human papillomavirus type 16 capsid proteins produced from recombinant Semliki Forest virus assemble into virus-like particles. Virology 214: 349–359, 1995
22. Sambrook JG, Russell DW: Molecular Cloning: a laboratory manual, 3rd Ed. Cold Spring Harbor Laboratory Press, Cold Spring Harbor, NY, 2001
23. Ghoshal K, Majumder S, Datta J, Motiwala T, Bai S, Sharma SM, Frankel W, Jacob ST: Role of human ribosomal RNA (rRNA) promoter methylation and of methyl-CpG-binding protein MBD2 in the suppression of rRNA gene expression. J Biol Chem 279: 6783–6793, 2004
24. Pfleiderer C, Smid A, Bartsch I, Grummt I: An undecamer DNA sequence directs termination of human ribosomal gene transcription. Nucleic Acids Res 18: 4727–4736, 1990
25. Zhao X, Rush M, Schwartz S: Identification of an hnRNP A1-dependent splicing silencer in the human papillomavirus type 16 L1 coding region that prevents premature expression of the late L1 gene. J Virol 78:10888–10905, 2004
26. Chen CY, You Y, Shyu AB: Two cellular proteins bind specifically to a purine-rich sequence necessary for the destabilization function of a c-fos protein-coding region determinant of mRNA instability. Mol Cell Biol 12: 5748–5757,1992
27. Schiavi SC, Wellington CL, Shyu AB, Chen CY, Greenberg ME, Belasco JG: Multiple elements in the c-fos protein-coding region facilitate deadenylation and decay by a mechanism coupled to translation. J Biol Chem 269: 3441–3448, 1994
28. Wisdom R, Lee W: The protein-coding region of c-myc mRNA contains a sequence that specifies rapid mRNA turnover and induction by protein synthesis inhibitors. Genes Dev 5: 232–243, 1991
29. Bachurski CJ, Theodorakis NG, Coulson RM, Cleveland DW: An amino-terminal tetrapeptide specifies cotranslational degradation of beta-tubulin but not alpha-tubulin mRNAs. Mol Cell Biol 14: 4076–4086, 1994
30. Zheng X, Kelley K, Elnakat H, Yan W, Dorn T, Ratnam M: mRNA instability in the nucleus due to a novel open reading frame element is

a major determinant of the narrow tissue specificity of folate receptor alpha. Mol Cell Biol 23: 2202–2212, 2003
31. Vannice JL, Taylor JM, Ringold GM: Glucocorticoid-mediated induction of alpha 1-acid glycoprotein: Evidence for hormone-regulated RNA processing. Proc Natl Acad Sci USA 81: 4241–4245, 1984
32. Narayan P, Towle HC: Stabilization of a specific nuclear mRNA precursor by thyroid hormone. Mol Cell Biol 5: 2642–2646, 1985
33. Vaessen RTM, Houweling A, Van der Eb AJ: Post-transcriptional control of class I MHC mRNA expression in adenovirus 12-transformed cells. Science 235: 1486–1488, 1987
34. Leys EJ, Crouse GF, Kellems RE: Dihydrofolate reductase gene expression in cultured mouse cells is regulated by transcript stabilization in the nucleus. J Cell Biol 99: 180–187, 1984
35. Tobler A, Miller CW, Johnson KR, Selsted ME, Rovera G, Koeffler HP: Regulation of gene expression of myeloperoxidase during myeloid differentiation. J Cell Physiol 136: 215–225, 1988
36. Akahane K, Pluznik DH: Interleukin-4 inhibits interleukin-1 alpha-induced granulocyte-macrophage colony-stimulating factor gene expression in a murine B-lymphocyte cell line via downregulation of RNA precursor. Blood 79: 3188–3195, 1992
37. Meskini RE, Boudouresque F, Ouafik L: Estrogen regulation of peptidylglycine {alpha}-amidating monooxygenase messenger ribonucleic acid levels by a nuclear posttranscriptional event. Endocrinology 138: 5256–5265, 1997

THE JOURNAL OF BIOLOGICAL CHEMISTRY VOL. 281, NO. 30, pp. 20788–20800, July 28, 2006


# Ubiquitination and Proteasome-dependent Degradation of Human Eukaryotic Translation Initiation Factor 4E*[S]

Received for publication, January 19, 2006, and in revised form, May 11, 2006 Published, JBC Papers in Press, May 23, 2006, DOI 10.1074/jbc.M600563200

Takayuki Murata[1] and Kunitada Shimotohno[2]

*From the Department of Viral Oncology, Institute for Virus Research, Kyoto University, Sakyo-ku, Kyoto 606-8507, Japan*

**Translation initiation factor 4E (eIF4E) is a cytoplasmic cap-binding protein that is required for cap-dependent translation initiation. Here, we have shown that eIF4E is ubiquitinated primarily at Lys-159 and incubation of cells with a proteasome inhibitor leads to increased eIF4E levels, suggesting the proteasome-dependent proteolysis of ubiquitinated eIF4E. Ubiquitinated eIF4E retained its cap binding ability, whereas eIF4E phosphorylation and eIF4G binding were reduced by ubiquitination. The W73A mutant of eIF4E exhibited enhanced ubiquitination/degradation, and 4E-BP overexpression protected eIF4E from ubiquitination/degradation. Because heat shock or the expression of the carboxyl terminus of heat shock cognate protein 70-interacting protein (Chip) dramatically increased eIF4E ubiquitination, Chip may be at least one ubiquitin E3 ligase responsible for eIF4E ubiquitination.**

The eukaryotic mRNA cap ($m^7$GTP) is a highly conserved structure located at the 5′-end of RNA molecule that plays an essential role in regulating mRNA decay, compartmentalization, maturation, and translation initiation (1). In the cytoplasm, eukaryotic translation initiation factor 4E (eIF4E)[3] specifically binds the mRNA cap structure and regulates cap-dependent translation initiation as a component of the eIF4F complex, which also includes the docking protein eIF4G and the ATP-dependent helicase eIF4A (2–4). The eIF4F complex enhances the assembly of the other initiation factors, such as eIF3, mitogen-activated protein kinase (MAPK) signal-integrating kinase, and the 40 S ribosomal subunit. Disruption or overproduction of eIF4E leads to aberrant cell growth or oncogenesis (4), demonstrating the importance of its availability for cellular protein synthesis.

Despite the importance of eIF4E, little is known about the regulation of eIF4E protein expression levels. Transcription of the gene is induced in response to serum, growth factors (5), or immunological activation in T cells (6). Additionally, cellular differentiation state also affects levels of the protein (7, 8). The eIF4E promoter contains two c-Myc-binding sites (9) and a heterogeneous nuclear ribonucleoprotein K-binding site (10), both of which are critical for the transcriptional regulation of eIF4E. However, the rate and mechanism of eIF4E degradation remain unclear, except that Othumpangat *et al.* (11) reported that eIF4E is ubiquitinated and degraded in a proteasome-dependent manner in response to heavy metal.

Ubiquitin (Ub), a low molecular weight polypeptide composed of 76 amino acids, can be covalently conjugated to Lys residues in target proteins (12, 13). Ub conjugation is a well coordinated event involving several classes of enzymes, including ubiquitin-activating enzymes (E1), ubiquitin-conjugating enzymes (E2), and ubiquitin ligases (E3). Protein ubiquitination is a signal for targeted recognition and ATP-dependent proteolysis by the 26 S proteasome. The Ub-proteasome pathway is an important factor controlling the expression and activity of regulatory proteins such as transcription factors or oncogenesis. Here, we have shown detailed analysis of eIF4E ubiquitination and proteasome-dependent degradation.

## EXPERIMENTAL PROCEDURES

*Cell Culture, Antibodies, and Reagents*—Human embryonic kidney (HEK) 293T cells were maintained in Dulbecco's modified Eagle's medium (Invitrogen) supplemented with 10% fetal bovine serum, 100 units/ml of nonessential amino acids (Invitrogen), and penicillin and streptomycin sulfate (Invitrogen). Rabbit anti-eIF4E and mouse anti-phospho-eIF4E antibodies were purchased from Cell Signaling Technology (Beverly, MA), and mouse anti-tubulin antibody was from Oncogene Research Products (San Diego, CA). Mouse anti-Myc antibody was from Santa Cruz Biotechnology (Santa Cruz, CA). Mouse and rabbit anti-FLAG antibodies were from Sigma. Mouse and rat anti-HA antibodies were obtained from Roche Applied Science. Horseradish peroxidase-linked goat antibodies to mouse or rabbit IgG were from Amersham Biosciences. Horseradish peroxidase-linked goat antibody to rat IgG was

* This work was supported in part by grants-in-aid for cancer research, by the second-term comprehensive 10-year strategy for cancer control, and by the Ministry of Health, Labor, and Welfare, as well as grants-in-aid for scientific research from the Ministry of Education, Culture, Sports, Science, and Technology, the Japanese Society for the Promotion of Science (JSPS), and the Program for Promotion of Fundamental Studies in Health Science of the Organization for Pharmaceutical Safety and Research of Japan. The costs of publication of this article were defrayed in part by the payment of page charges. This article must therefore be hereby marked "*advertisement*" in accordance with 18 U.S.C. Section 1734 solely to indicate this fact.

[S] The on-line version of this article (available at http://www.jbc.org) contains supplemental Figs. S1 and S2.

[1] Recipient of a JSPS postdoctoral fellowship. Present address: Dept. of Biochemistry, McGill University, McIntyre Bldg., 3655 Sir William Osler, Montreal, H3G 1Y6 Quebec, Canada

[2] To whom correspondence should be addressed. Tel. 81-75-751-4000; Fax: 81-75-751-3998; E-mail: kshimoto@virus.kyoto-u.ac.jp.

[3] The abbreviations used are: eIF4E, eukaryotic translation initiation factor 4E; Hsc70, heat shock cognate protein 70; Chip, Hsc70-interacting protein; $m^7$GTP, 7-methyl guanosine triphosphate; MAPK, mitogen-activated protein kinase; Ub, ubiquitin; IP, immunoprecipitation; IB, immunoblotting; WCE, whole cell extracts; 4E-BP, eIF4E-binding protein; DPM, dolichol-phosphate-mannose; HEK, human embryonic kidney; IP, immunoprecipitation; IB, immunoblot; WT, wild type; E1, ubiquitin-activating enzyme; E2, ubiquitin carrier protein; E3, ubiquitin-protein isopeptide ligase; HA, hemagglutinin.

acquired from Jackson ImmunoResearch. MG132 was purchased from Peptide Institute (Osaka, Japan).

*Plasmid Construction*—For cloning human cDNAs, total RNA was prepared from HEK293T or Huh-7 cells and amplified by reverse transcription PCR. The coding region of human eIF4E was obtained and was cloned into the vector pcDNA3 or pcDNA3-FLAG (14) to generate pceIF4E or pcFLAGeIF4E, respectively. To prepare pcMycChip and pcMyc4E-BP1–3, the coding regions of human Chip and 4E-BP1–3 were amplified and cloned into pcDNA3-Myc (14). Primer sequences used were as follows. eIF4E, 5′-cg**gaattc**atggcgactgtcgaaccggaaacc-3′ (forward), 5′-ctga**ctcgag**ttaaacaacaaacctatttttag-3 (reverse). Chip, 5′-tatc**ggatcc**tgaagggcaaggaggagaaggag-3′ (forward), 5′-gat**ggatcc**tcagtagtcctccacccagccattc-3′ (reverse). 4E-BP1, 5′-ctatc**ggatcc**tgtccgggggcagcagctgcag-3′ (forward), 5′-cgat**ggatcc**taaatgtccatctcaaactgtg-3 (reverse). 4E-BP2, 5′-ctatc**ggatcc**tgtcctcgtcagccggcagcgg-3′ (forward), 5′-cgat**ggatcc**tcagatgtccatctcgaactgag-3 (reverse). 4E-BP3, 5′-ctatc**ggatcc**tgtcaacgtccactagctgccc-3′ (forward), 5′-cgat**ggatcc**ttagatgtccatttcaaattgtg-3 (reverse). Bold letters in the primers denote restriction sites. Expression plasmids for eIF4E point mutants were generated by PCR using pcFLAGeIF4E as a template. To create pcHAUb, the Ub gene was amplified by reverse transcription PCR and inserted into the BamHI site in the pcDNA3-HA (14).

*Immunoprecipitation/Immunoblotting*—HEK293T cells were transfected with appropriate plasmids using FuGENE 6 reagent (Roche Applied Science). For immunoprecipitation/immunoblotting to detect ubiquitinated forms of eIF4E, cells were solubilized 24 h post-transfection in 100 μl of SDS(+) lysis buffer (10 mM Tris-HCl, pH 7.8, 150 mM NaCl, 1 mM EDTA, 1% Nonidet P-40, 1% SDS, and protease inhibitor mixture). Lysates were boiled for 5 min to completely denature proteins and disrupt non-covalent interactions. Cell lysates were then diluted with 900 μl of SDS(−) lysis buffer (10 mM Tris-HCl, pH 7.8, 150 mM NaCl, 1 mM EDTA, 1% Nonidet P-40, and protease inhibitor mixture) and precleared with protein-G-Sepharose (Amersham Biosciences. Supernatants were then mixed with antibody and incubated at 4 °C for 1 h. Immunocomplexes were recovered by incubating protein-G-Sepharose for 1 h, and the resin was washed five times with SDS(−) lysis buffer. Samples were subjected to SDS-PAGE, followed by immunoblotting with indicated antibodies as described previously (15). For immunoprecipitation/immunoblotting to detect protein associations, SDS(−) lysis buffer was used and samples were not boiled before immunoprecipitation.

*$m^7$GTP-Sepharose Precipitation/Immunoblotting*—Hek293 cells were lysed in SDS(−) lysis buffer, precleared, incubated with 7-methyl GTP-Sepharose (Amersham Biosciences) at 4 °C for 2 h, and then washed extensively with the same buffer Precipitates were subjected to SDS-PAGE and immunoblotting as described above. For highly efficient exposure, we used Lumigen TMA-6 Solution (Amersham Biosciences).

## RESULTS

*Ubiquitination and Proteasome-dependent Degradation of eIF4E*—To confirm ubiquitination of eIF4E in cells, we transfected HEK293T cells with FLAG-tagged eIF4E (pcFLAGeIF4E) and/or HA-tagged Ub (pcHAUb). Cellular proteins were then subjected to immunoprecipitation (*IP*) with anti-FLAG antibody, followed by immunoblotting (*IB*) with anti-HA antibody (Fig. 1*A*, *top panel*). When both eIF4E and Ub were produced, mono- (eIF4E-Ub) or poly- (eIF4E-$Ub_n$) ubiquitinated forms of eIF4E appeared (Fig. 1*A*, *top panel*, *lane 4*). The *arrows* in Fig. 1 depict the estimated size for non-ubiquitinated eIF4E. Ubiquitination was not detectable when either eIF4E or Ub alone was expressed (Fig. 1*A*, *top panel*, *lanes 2* and *3*), demonstrating the specific linkage of Ub and eIF4E. The membrane was stripped and probed with anti-FLAG antibody to confirm the successful precipitation of eIF4E protein (Fig. 1*A*, *2nd panel*). Additionally, all transfected proteins were expressed and gels were loaded equally as shown in Fig. 1*A*, *3rd*, *4th*, and *bottom panels*. Non-ubiquitinated FLAGeIF4E protein resolved around 27 kDa and the mono-ubiquitinated form was ~37 kDa. Additionally, we were able to detect mono-ubiquitinated eIF4E in whole cell extracts (*WCE*) (Fig. 1*B*, *top panel*, *lane 3*).

The ubiquitination of eIF4E may be affected by its phosphorylation, cap binding, and eIF4G binding. We generated mutant forms of eIF4E to further examine this issue (Fig. 1*C*). We mutated Ser-209, the eIF4E residue phosphorylated by MAPK signal-integrating kinase (16), Trp-56, a residue located within the eIF4E hydrophobic pocket, required for cap binding (17), and Trp-73, a residue essential for the interaction of eIF4E with eIF4G/4E-BP (18). Although the ubiquitination of either S209A or W56A eIF4E was comparable with that seen with WT eIF4E, the ubiquitination of the W73A mutant was dramatically increased (Fig. 1*C*, *top panel*, *lane 6*), suggesting a role of eIF4G/4E-BP association in regulating eIF4E ubiquitination.

Ubiquitinated proteins are typically degraded by the proteasome, and we used MG132, a proteasome inhibitor, to examine whether eIF4E was degraded in this manner (Fig. 1, *D* and *E*). When cells co-transfected with pcFLAGeIF4E and pcHAUb were treated with MG132 for 12 h, we observed the accumulation of polyubiquitinated forms of eIF4E (Fig. 1*D*, *top panel*, *lane 4*). Mono-ubiquitinated eIF4E became less prominent with MG132 (Fig. 1*D*, *top panel*, *lane 4*), presumably because of the accumulation of other ubiquitinated target proteins.

Although the levels of eIF4E mutants were almost comparable at 24 h after transfection (*e.g.* Fig. 1*C*, *middle panel*), the band for W73A eIF4E became very faint when incubated for 48 h (Fig. 1*E*, *lane 4*) or more (not shown). We assume the shorter half-life of the mutant protein is relevant to the enhanced ubiquitination (Fig. 1*C*, *top panel*, *lane 6*). At 24 h, degradation of the protein is not evident because it is compensated by the massive production from efficient plasmid vector, whereas at 48 h, the production becomes weaker and the degradation becomes apparent (see "Discussion").

Treatment with MG132 increased levels of both WT and W73A mutant eIF4E (Fig. 1*E*). MG132 was added at 24 h after transfection because it is toxic for cells when administered for more than 24 h. These results clearly demonstrate that eIF4E is ubiquitinated and degraded in a proteasome-dependent manner and suggest that the interaction of eIF4E with eIF4G/4E-BP is important for the regulation of eIF4E ubiquitination/degradation.

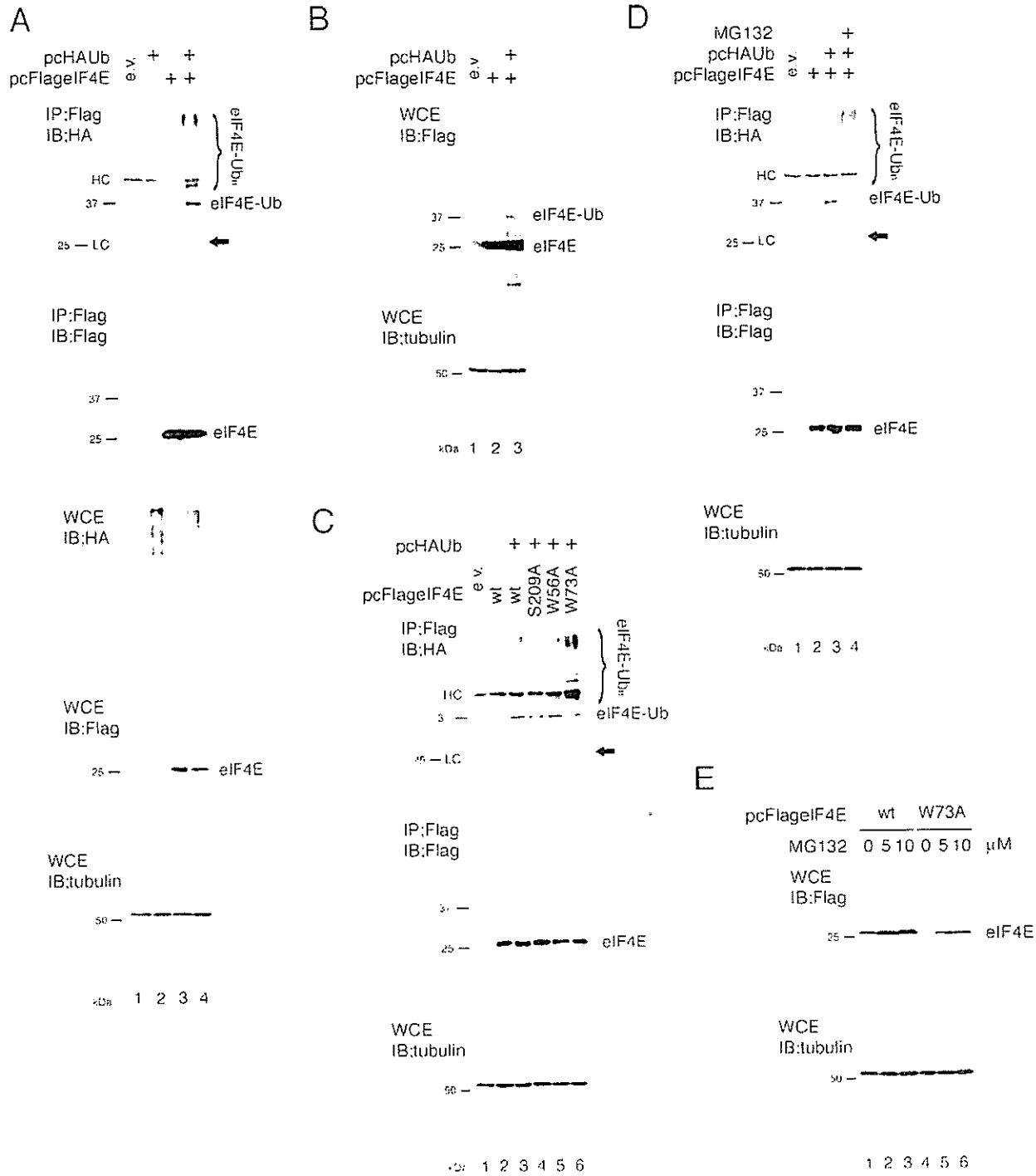


FIGURE 1 **Ubiquitination and proteasome-dependent degradation of eIF4E.** *A*, ubiquitination of eIF4E. HEK293T cells were transfected with pcFLAGeIF4E and/or pcHAUb. 24 h after transfection, cell lysates were immunoprecipitated (*IP*) with anti-FLAG antibody. The immunoprecipitates were subjected to SDS-PAGE and analyzed by immunoblotting (*IB*) with anti-HA antibody (*top panel*). The membrane was then stripped and reprobed with anti-FLAG antibody (*2nd panel*). A portion of the whole cell extracts (*WCE*) was directly subjected to SDS-PAGE, and IB was performed with anti-HA (*3rd panel*), FLAG (*4th panel*), or tubulin (*bottom panel*) antibody. *B*, detection of eIF4E ubiquitination without IP. Cells transfected with pcFLAGeIF4E and/or pcHAUb were subjected to SDS-PAGE, followed by IB with anti-FLAG (*upper*) or tubulin (*lower*) antibody. The upper panel was overexposed to detect mono-ubiquitinated eIF4E. *C*, effect of mutations on ubiquitination. Cells transfected with pcHAUb and/or wild-type (*WT*) pcFLAGeIF4E or the mutant forms of pcFLAGeIF4E were lysed for IP with anti-FLAG antibody, followed by IB with anti-HA antibody (*top*). The membrane was then stripped and reprobed with anti-FLAG antibody (*middle*). Levels of tubulin in the WCE were examined as a loading control (*bottom*). *D*, effect of MG132 on eIF4E ubiquitination..24 h after transfection, cells were treated with MG132 or $Me_2SO$. At 12 h after the addition of MG132, cells were harvested for IP with anti-FLAG antibody, followed by IB with anti-HA antibody (*top*). The membrane was then stripped and reprobed with anti-FLAG antibody (*middle*). Tubulin was used as a loading control (*bottom*). *E*, effect of MG132 on eIF4E levels. Cells were transfected with WT or W73A mutant of pcFLAGeIF4E. 24 h after transfection, cells were treated with MG132 (5, 10 μM) and incubated for another 24 h. WCE was subjected to SDS-PAGE and IB with anti-FLAG (*upper*) or tubulin (*bottom*) antibody. *HC* and *LC* denote bands for IgG heavy chain and light chain. *e.v.*, empty vector. *Arrow*, estimated size for non-ubiquitinated eIF4E. *eIF4E-Ub*, mono-ubiquitinated eIF4E; *eIF4E-Ub$_n$*, polyubiquitinated eIF4E.

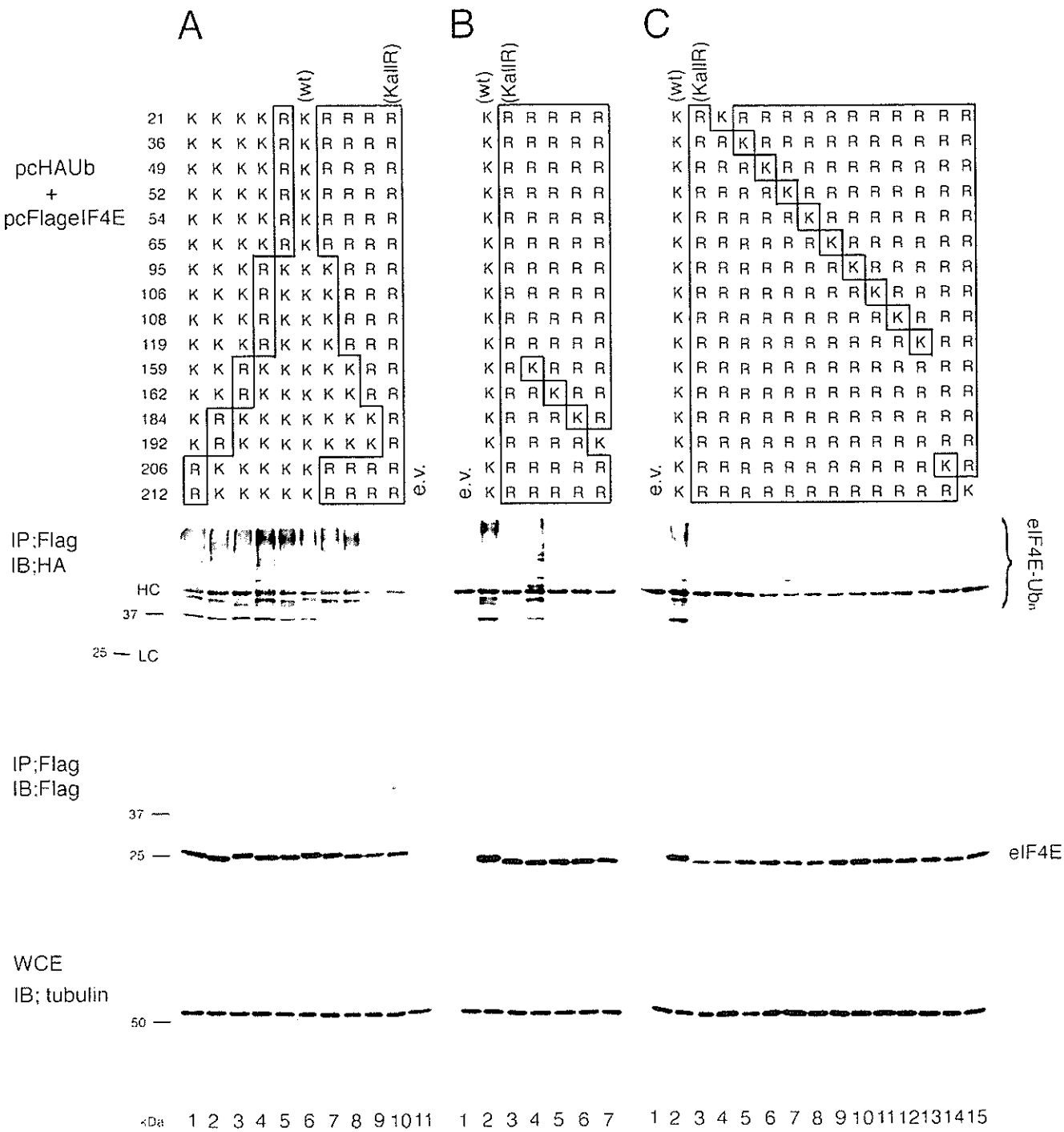


FIGURE 2. **Identification of the ubiquitinated residue.** *A–C*, as in Fig. 1*A*, cells were transfected with pcHAUb and WT or mutant forms of pcFLAGeIF4E. 24 h after transfection, cell lysates were subjected to IP with anti-FLAG antibody, followed by SDS-PAGE and IB with anti-HA antibody (*upper panel*). The membrane was then stripped and reprobed with anti-FLAG antibody (*middle*). Levels of tubulin in the WCE serve as a control (*bottom*).

*Identification of Residues Required for eIF4E Ubiquitination*—Target proteins are ubiquitinated on Lys residues, and eIF4E contains 16 Lys residues. To identify the particular residue(s) that become ubiquitinated, we generated a series of Lys to Arg (K/R) mutants (Fig. 2*A*, *lanes 1–5*). However, none of these 5 K/R mutants exhibited decreased ubiquitination compared with WT eIF4E, suggesting that multiple Lys residues may be ubiquitinated. Therefore, we next prepared an expression construct, pcFLAGeIF4EKallR, in which all Lys residues were mutated to Arg (Fig. 2*A*, *lane 10*), and, as expected, this mutant was hardly ubiquitinated.

We subsequently generated 16 plasmids in which a single Lys residue of the KallR mutant was restored while the other Lys residues remained mutated (Fig. 2*B*, *lanes 4–7*, Fig. 2*C*, *lanes 3–15*).

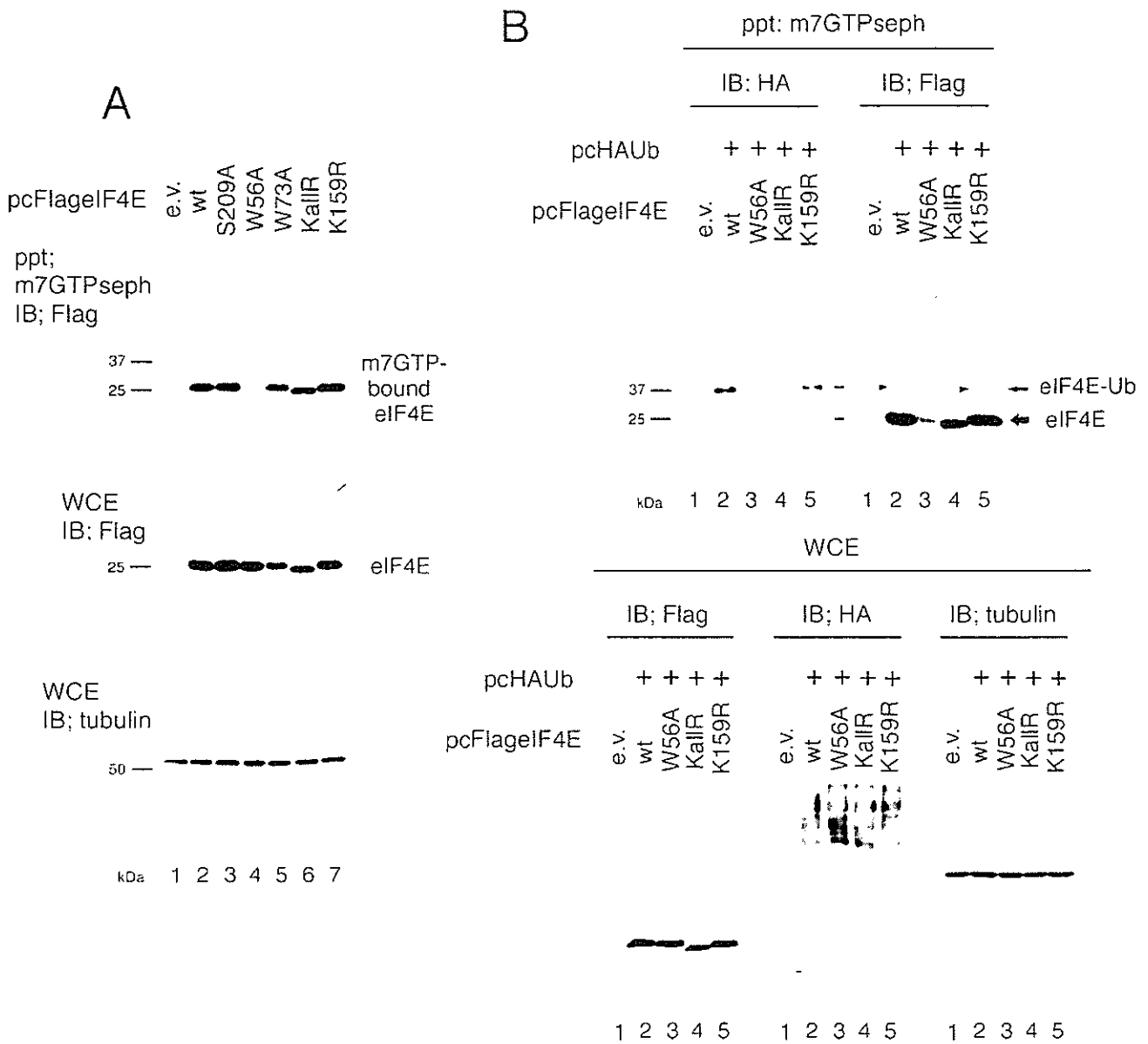


FIGURE 3. **$m^7$GTP association of eIF4E.** *A*, association of eIF4E mutants and $m^7$GTP. Cells transfected with WT or mutant forms of pcFLAGeIF4E were lysed 24 h after transfection. Lysates were precipitated with $m^7$GTP-Sepharose and subjected to SDS-PAGE and IB with anti-FLAG antibody (*top*). As control, a portion of the WCE was directly subjected to SDS-PAGE, and IB was performed with anti-FLAG (*middle*) or tubulin (*bottom*) antibody. *B*, ubiquitinated eIF4E associated with $m^7$GTP. Cells transfected with WT or mutant forms of pcFLAGeIF4E and pcHAUb were lysed 24 h after transfection. $m^7$GTP-associated proteins were collected and subjected to IB with anti-HA (*upper left panel*) or FLAG (*upper right panel*) antibody. As controls, levels of eIF4E (*lower left panel*), Ub (*lower middle*), and tubulin (*lower right*) in the WCE were examined with anti-FLAG, HA, and tubulin antibodies, respectively.

Interestingly, restoration of a single Lys, Lys-159, restored the ubiquitination of eIF4E to the same extent as WT (Fig. 2*B*, *lanes 2* and *4*). Thus, it is likely that Ub conjugation occurs primarily at Lys-159, although other Lys residues become Ub modified in the absence of this residue (Fig. 2*A*, *lane 3*).

*Effect of eIF4E Ubiquitination on $m^7$GTP Association*—Because cap binding is essential for eIF4E function, we examined eIF4E $m^7$GTP binding using $m^7$GTP-Sepharose (Fig. 3). FLAG-tagged eIF4E mutants were expressed in cells, and $m^7$GTP-binding proteins were precipitated, followed by detection by IB. As expected, a W56A eIF4E mutant only weakly associated with $m^7$GTP (Fig. 3*A*, *lane 4*) (17), but the other eIF4E mutants examined, including KallR and K159R, all bound $m^7$GTP as efficiently as WT eIF4E (Fig. 3*A*).

We next wished to examine whether ubiquitinated eIF4E was capable of binding the cap structure. Cells were transfected with pcFLAGeIF4E mutants together with pcHAUb, and $m^7$GTP-bound proteins were detected using anti-HA (Fig. 3*B*, *upper left panel*) and anti-FLAG (*upper right panel*) antibodies. The anti-HA antibody detected both mono-and polyubiquitinated proteins (Fig. 3*B*, *upper left*, *lanes 2* and *5*), and when precipitated material was blotted with anti-FLAG at least mono-ubiquitinated WT and K159R eIF4E were seen (Fig. 3*B*, *upper right*, *lanes 2* and *5*, *arrowhead*). Protein expression was

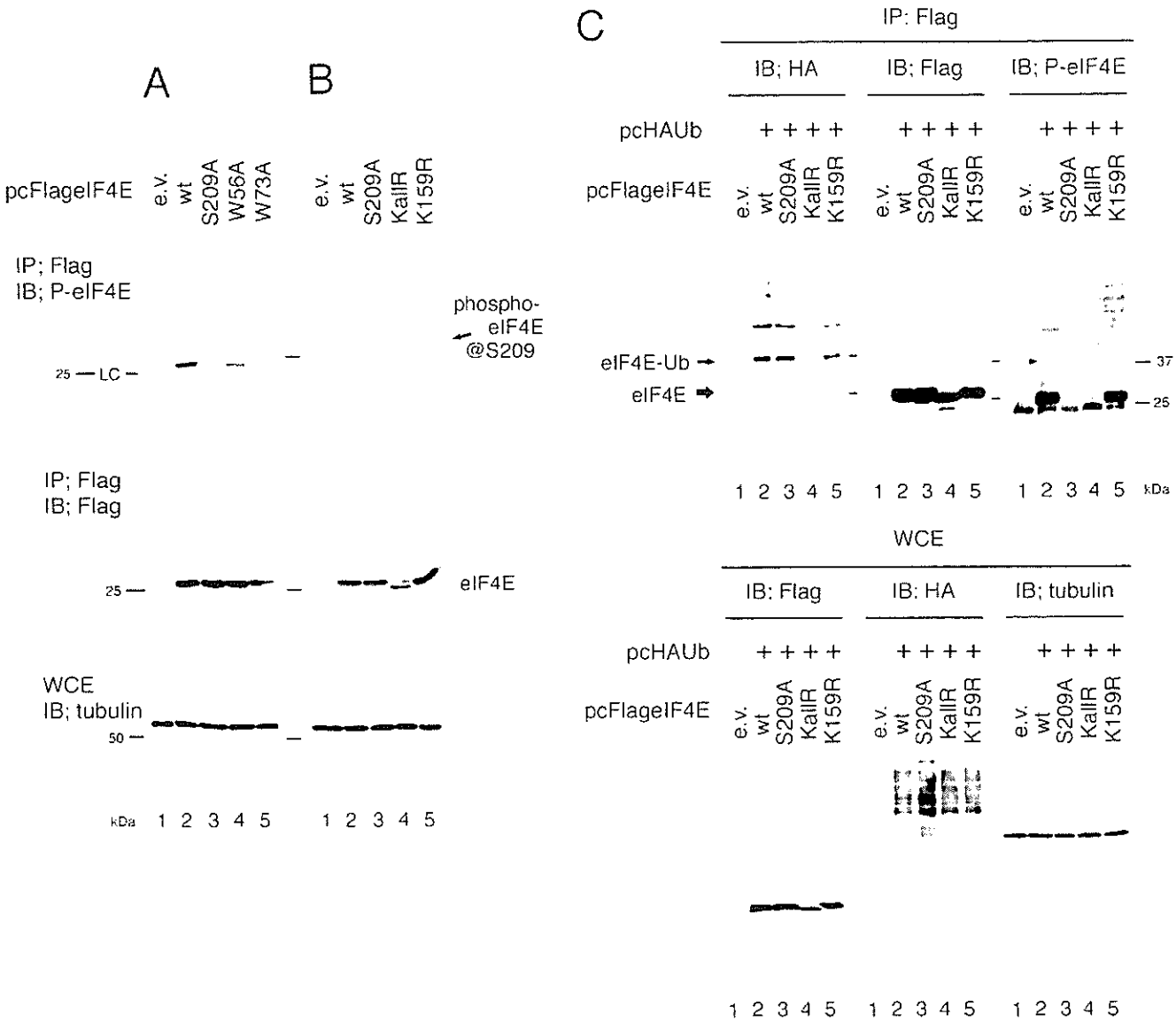


FIGURE 4. **Phosphorylation of eIF4E.** *A* and *B*, phosphorylation of eIF4E mutants. Cells transfected with WT or mutant forms of pcFLAGeIF4E were lysed 24 h after transfection. Lysates were precipitated with anti-FLAG antibody and subjected to IB with anti-phospho-eIF4E (*top panels*) or FLAG (*middle*) antibody. As a control, levels of tubulin in the WCE were examined (*bottom*). *C*, phosphorylation of ubiquitinated eIF4E was not detectable. Lysates from cells transfected with WT or mutant forms of pcFLAGeIF4E and pcHAUb were precipitated with anti-FLAG antibody and subjected to SDS-PAGE and IB with anti-HA (*upper left panel*), FLAG (*upper middle*) or phospho-eIF4E (*upper right*) antibody. As controls, levels of eIF4E (*lower left*), Ub (*lower middle*), or tubulin (*lower right*) in the WCE were examined using anti-FLAG, HA, or tubulin antibody, respectively.

confirmed in the lower panels of Fig. 3*B*. Ubiquitinated W56A and KallR eIF4E were not precipitated with $m^7GTP$ (Fig. 3*B*, *upper panels*, *lanes 3* and *4*), because the cap binding and ubiquitination of W56A and KallR mutants, respectively, are very low. Thus, these results suggest that ubiquitinated eIF4E remains capable of binding the cap structure.

*Effect of eIF4E Ubiquitination on Phosphorylation*—We next wished to examine the possible relationship between eIF4E ubiquitination and phosphorylation, and we used a phospho-eIF4E antibody for these studies. As expected, this antibody did not react with the phosphorylation mutant S209A, although the WT and W56A mutants were phosphorylated (Fig. 4*A*, *top panel*, *lanes 2–4*). W73A also failed to be phosphorylated (Fig. 4*A*, *top panel*, *lane 5*). This is consistent with published reports indicating that MAPK signal-integrating kinase, the kinase responsible for eIF4E phosphorylation, is recruited by eIF4G (18). The KallR mutant showed little or no phosphorylation, whereas levels of K159R phosphorylation were normal (Fig. 4*B*, *top panel*, *lanes 4* and *5*).

We next examined whether ubiquitinated eIF4E was phosphorylated. As depicted in the *upper right panel* of Fig. 4*C*, despite gross overexposure, mono-ubiquitinated eIF4E was not seen to be phosphorylated (Fig. 4*C*, *upper right*, *lane 2*, *arrowhead*), whereas ubiquitination of eIF4E in the same samples was evident when blotted with anti-HA or anti-FLAG antibodies (Fig. 4*C*, *upper left* and *middle panels*). Some faint bands were visible above 37 kDa in Fig. 4*C* (*upper right panel*), but we assume these are nonspecific. Therefore, we conclude that phosphorylation

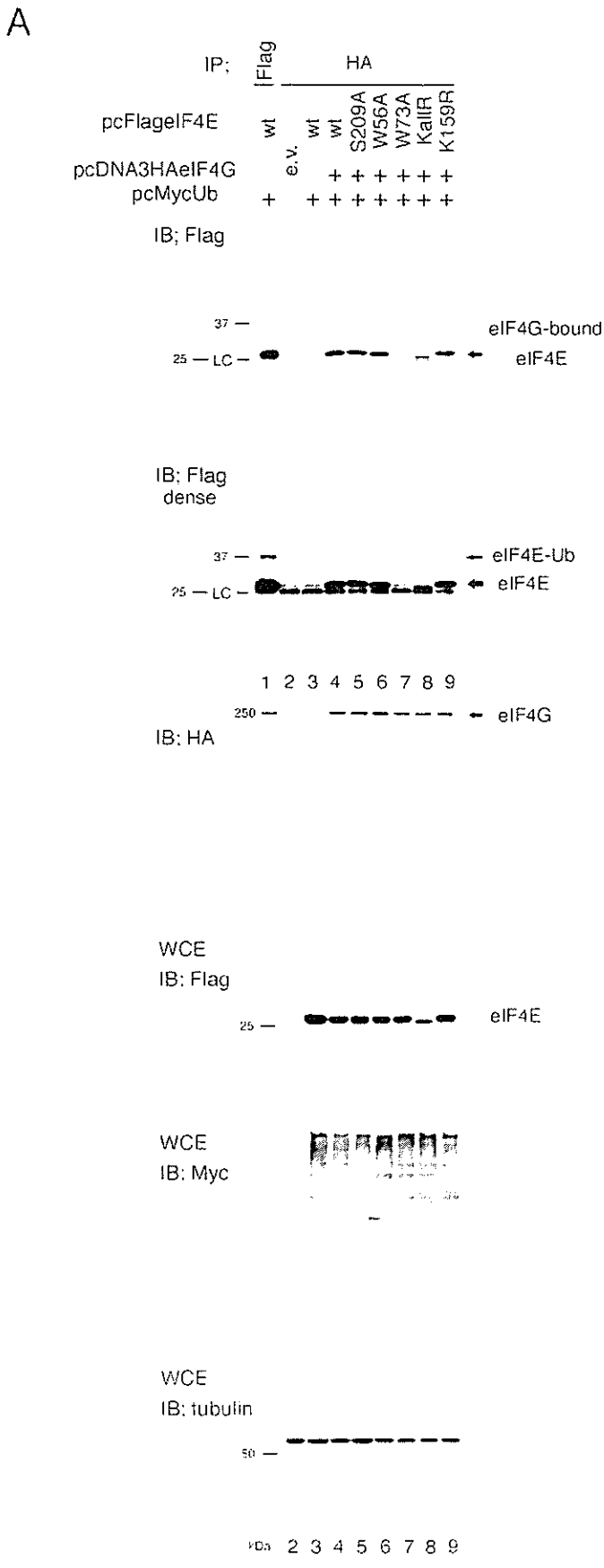

and ubiquitination may not occur simultaneously in a single eIF4E molecule. However, we cannot exclude the possibility that levels of eIF4E phosphorylation are very low if the molecule is modified with Ub.

*Effect of eIF4E Ubiquitination on eIF4G Binding*—Because the association of eIF4E with eIF4G is essential for cap-mediated translation initiation, we analyzed the binding of eIF4E to eIF4G by IP and IB. HA-tagged eIF4G and FLAG-tagged eIF4E mutants were produced in cells, together with Myc-tagged Ub. eIF4G was isolated with anti-HA antibody, and eIF4G-associated eIF4E was detected with anti-FLAG antibody (Fig. 5*A*, *top*, *2nd panel*). Membranes were stripped and reprobed with anti-HA antibody (Fig. 5*A*, *3rd panel*). When WT FLAG-tagged eIF4E was co-expressed with eIF4G and Ub, only non-ubiquitinated eIF4E co-precipitated with eIF4G, even upon gross overexposure of the blot (Fig. 5*A*, *1st* and *2nd panels*, *lanes 4–9*). As expected, the W73A mutant of eIF4E did not associate with eIF4G, but the association of KallR mutant with eIF4G was also weak (Fig. 5*A*, *top panel*, *lanes 7* and *8*). As a control, we expressed FLAG-tagged WT eIF4E with Myc-tagged Ub and precipitated total eIF4E with anti-FLAG. As seen in Fig. 5*A*, *2nd panel*, *lane 1*, at least mono-ubiquitinated eIF4E was detectable under these conditions, but ubiquitinated eIF4E was not found in the eIF4G-associated fractions (Fig. 5*A*, *2nd panel*, *lanes 4–9*). As an additional control, we confirmed that the expression of eIF4G did not suppress eIF4E ubiquitination (Fig. 5*B*, *top panel*, *lane 3*). Thus, it is likely that eIF4G does not bind ubiquitinated forms of eIF4E with any appreciable affinity.

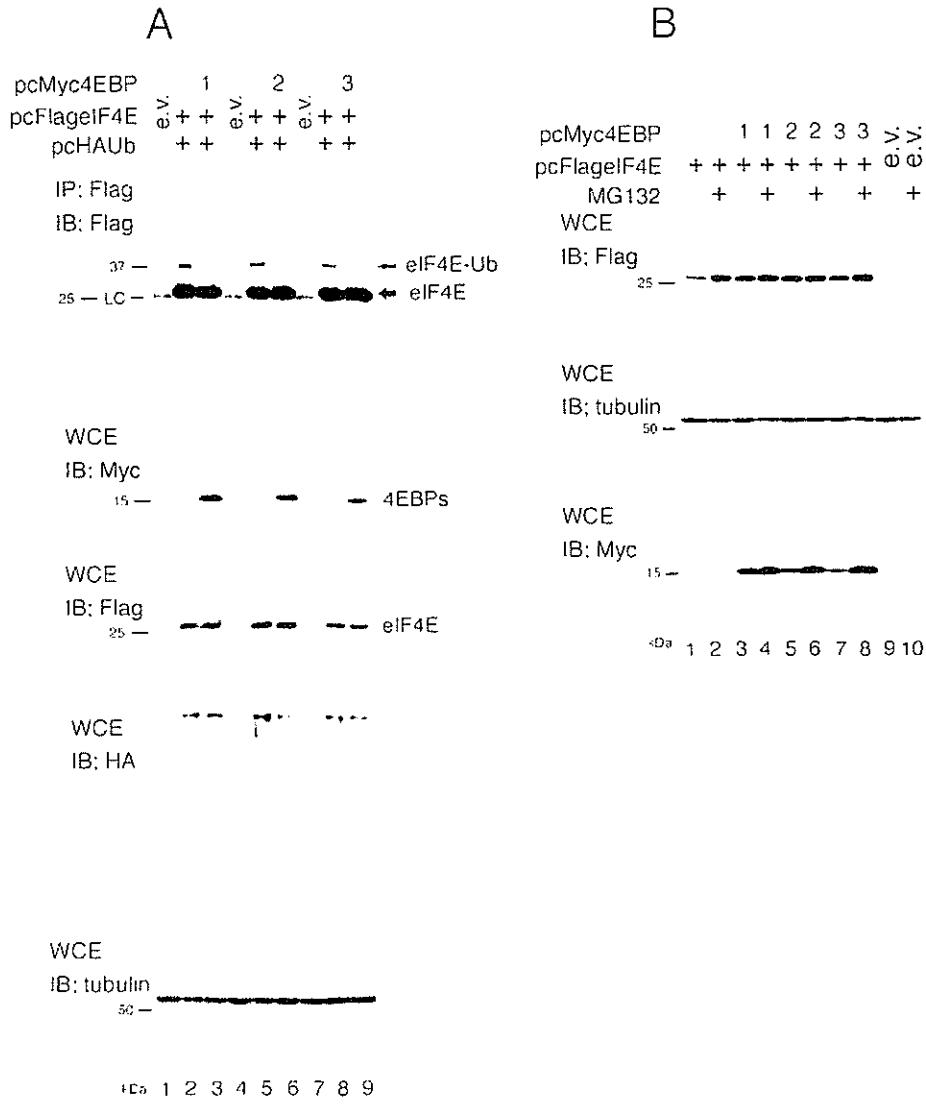


FIGURE 6. **Effect of 4E-BP on eIF4E ubiquitination/degradation.** *A*, expression of 4E-BP suppressed eIF4E ubiquitination. Cell lysates transfected with pcFLAGeIF4E, pcHAUb, and pcMyc4E-BP1, 2, or 3 were precipitated with anti-FLAG antibody and subjected to IB with anti-FLAG (*top panel*) antibody. Levels of 4E-BP (*2nd panel*), eIF4E (*3rd*), Ub (*4th*), or tubulin (*bottom*) in the WCE were checked using anti-Myc, FLAG, HA, or tubulin antibody, respectively. *B*, expression of 4E-BP suppressed eIF4E degradation. Cells were transfected with pcFLAGeIF4E and/or pcMyc4E-BP1, 2, or 3. 24 h after transfection, cells were treated with MG132 (10 μM) and incubated for another 24 h. WCE was subjected to SDS-PAGE and IB with anti-FLAG (*upper*), tubulin (*middle*), or Myc (*bottom*) antibody.

*4E-BP Binding Suppresses eIF4E Ubiquitination and Degradation*—4E-BP proteins bind eIF4E and negatively regulate cap-dependent translation initiation. To examine whether 4E-BP affects the ubiquitination of eIF4E, three 4E-BP isoforms were cloned, Myc tagged, and transfected into cells with Ub and eIF4E. Although mono-ubiquitinated eIF4E was clearly detected in the absence of 4E-BP (Fig. 6*A*, *lanes 2*, *5*, and *8*), 4E-BP production eliminated the observed ubiquitination (*lanes 3*, *6*, and *9*). Additionally, only non-ubiquitinated eIF4E was associated with 4E-BP (supplemental Fig. S1).

FIGURE 5. **eIF4G association of eIF4E.** *A*, association between eIF4E mutants and eIF4G. Lysates from cells transfected with WT or mutant forms of pcFLAGeIF4E, pcDNA3HAeIF4G, and pcMycUb were precipitated with anti-HA antibody (*lanes 2–9*) and subjected to IB with anti-FLAG (*top* and *2nd panels*) or HA (*3rd panel*) antibody. To assess ubiquitination levels of eIF4G-associated eIF4E, the membrane in the top panel was overexposed in the 2nd panel. For *lane 1*, cell lysates transfected with pcFLAGeIF4E and pcMycUb were precipitated with anti-FLAG antibody and loaded for the *top* and *2nd panels* to examine the levels of eIF4E ubiquitination. Levels of eIF4E (*4th panel*), Ub (*5th panel*), or tubulin (*bottom panel*) in the WCE were checked using anti-FLAG, Myc, or tubulin antibody, respectively. *B*, effect of eIF4G overexpression on eIF4E ubiquitination. Lysates from cells transfected with WT pcFLAGeIF4E, pcDNA3HAeIF4G, and/or pcMycUb were precipitated with anti-FLAG antibody and subjected to IB with anti-FLAG (*top panel*) antibody. Levels of eIF4G (*2nd panel*), eIF4E (*3rd*), Ub (*4th*), or tubulin (*bottom*) in the WCE were assessed using anti-HA, FLAG, Myc, or tubulin antibody, respectively.

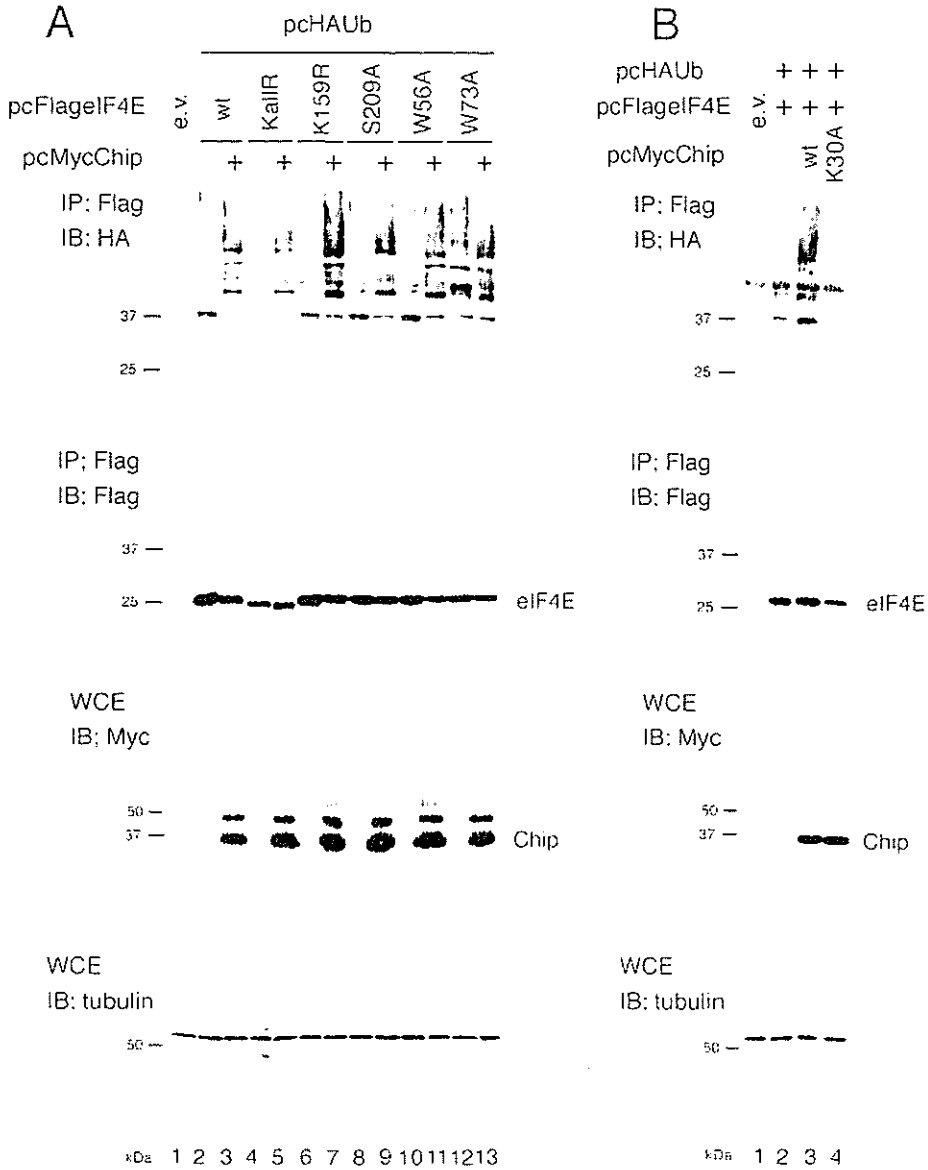


FIGURE 7. **Increased ubiquitination of eIF4E by Chip.** *A*, Chip enhanced eIF4E ubiquitination. Cells were transfected with pcHAUb and mutant forms of pcFLAGeIF4E, with/without pcMycChip. 24 h after transfection, cell lysates were subjected to IP with anti-FLAG antibody, followed by IB with anti-HA antibody (*top panel*). The membrane was then stripped and reprobed with anti-FLAG antibody (*2nd panel*). The WCE was subjected to IB with anti-Myc (*3rd panel*) or tubulin (*bottom panel*) antibody. *B*, importance of the interaction between Hsc70 and Chip. IP/IB was performed in parallel with *panel A*, except the K30A mutant was tested in *lane 4*.

We next determined whether 4E-BP expression affected eIF4E degradation (Fig. 6*B*). As depicted in Fig. 1*E*, eIF4E protein levels were lower in the absence of MG132 (Fig. 6*B*, *top panel, lane 1*), whereas levels were increased by the addition of MG132 (Fig. 6*B*, *top panel, lane 2*). Interestingly, when 4E-BP1, 2, or 3 was co-expressed, eIF4E levels in the absence of MG132 (Fig. 6*B*, *top panel, lanes 3, 5,* and *7*) were almost comparable with those with the inhibitor (Fig. 6*B*, *top panel, lanes 4. 6,* and *8*), suggesting that 4E-BP proteins inhibit the degradation of eIF4E. Taken together with the observation that the W73A mutant shows enhanced ubiquitination, these data strongly suggest that 4E-BP binding negatively regulates eIF4E ubiquitination and degradation.

*Chip-enhanced eIF4E Ubiquitination*—Ubiquitination requires the concerted action of a series of enzymes, and actual Ub addition is performed by E3 ligases. We wished to determine the E3 ligase responsible for eIF4E ubiquitination, and we tested Chip, a well characterized E3 ligase. When cells were co-transfected with Chip and WT, S209A, W56A, and K159R eIF4E mutants, we observed the enhanced ubiquitination of all constructs (Fig. 7*A*, *top panel*). Additionally, KallR was ubiquitinated when Chip was co-expressed in cells (Fig. 7*A*, *lane 5*). Because there were no Lys residues in this eIF4E mutant, we speculate that the amino-terminal Met residue of this protein may be ubiquitinated (19) or that the FLAG epitope contains a Lys residue that could be Ub modified. Ubiquitination of the W73A mutant was not clearly increased (Fig. 7*A*, *lane 13*), but ubiquitination levels of this mutant are likely saturated. A K30A Chip mutant that is unable to interact with Hsc70 (20) did not enhance eIF4E ubiquitination (Fig. 7*B*, *lane 4*), whereas WT Chip did (*lane 3*).

We next wished to determine whether eIF4E and Chip directly interacted by IP/IB. As shown in Fig. 8*A*, all forms of eIF4E examined interacted with Chip (Fig. 8*A*, *top panel, lanes 3–8*). Interestingly, eIF4E did not associate with the K30A Chip mutant (Fig. 8*B*, *lane 4*), suggesting that Chip associates with eIF4E via Hsc70. These data indicate that eIF4E can be ubiquitinated by Chip, possibly in an Hsc70-dependent manner

*Heat Shock-enhanced eIF4E Ubiquitination*—Cells respond to certain stimuli through regulating protein synthesis levels (21, 22). Generally, under conditions of cell stress or apoptosis, cap-mediated translation is suppressed, whereas cap-independent, internal ribosome entry site-dependent translation increases. To clarify whether eIF4E ubiquitination plays a role in regulating these changes, we first examined levels of ubiquitination in heat shocked cells (Fig. 9*A*). When cells were heat shocked (45 °C, 10 min), Ub conjugation became evident 2 h after heat shock (Fig. 9*A*, *top panel, lane 4*), and levels then returned to normal after 4–8 h (Fig. 9*A*, *lanes 6, 8,* and *10*). Heat shock also induced KallR mutant ubiquitination (Fig. 9*B*, *top panel, lane 7*).

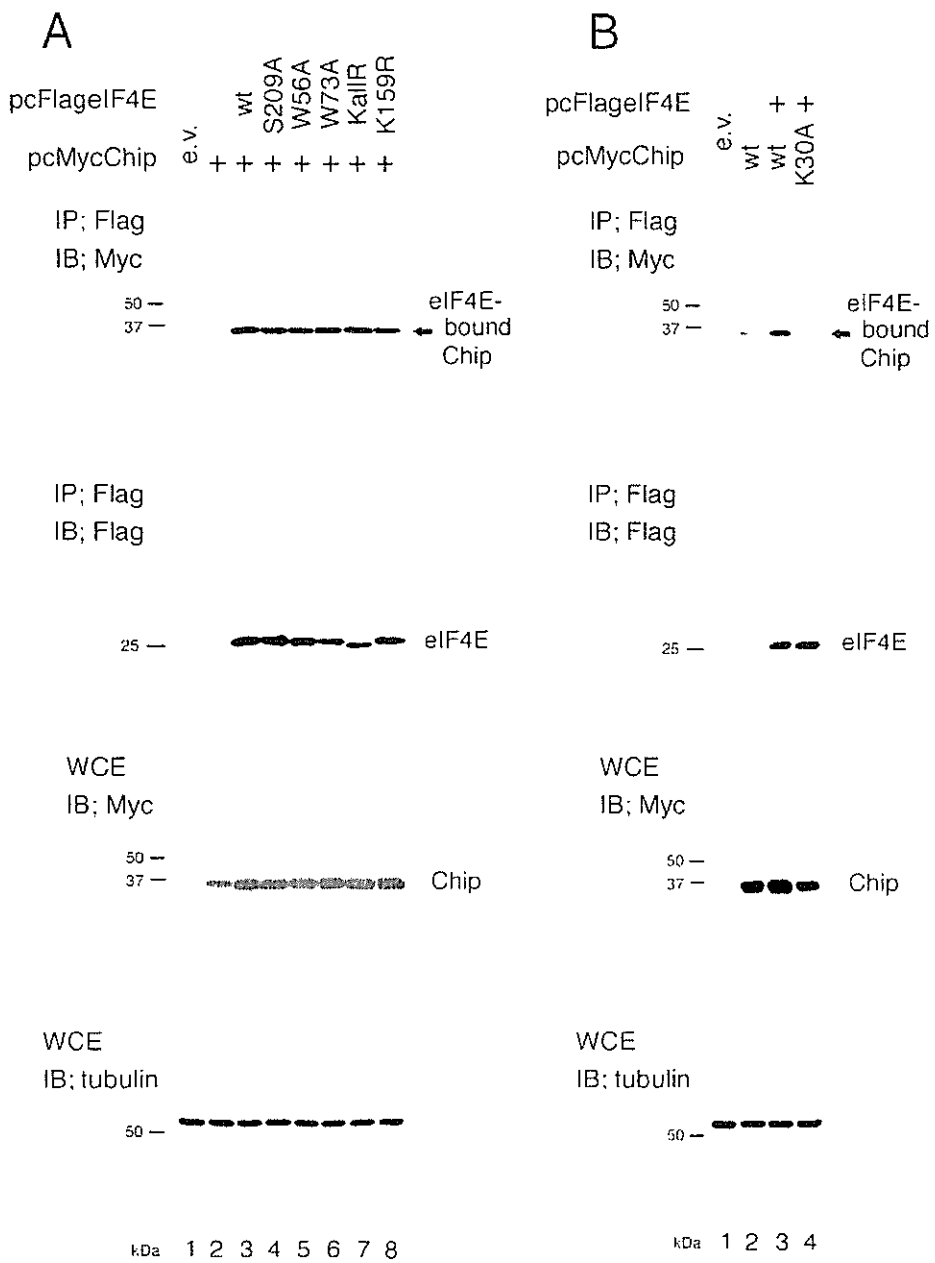


FIGURE 8. **Association of eIF4E and Chip.** *A* and *B*, cells were transfected with WT or mutant forms of pcFLAGeIF4E and pcMycChip. 24 h after transfection, cell lysates were subjected to IP with anti-FLAG antibody, followed by IB with anti-Myc antibody (*top panels*). The membrane was then stripped and reprobed with anti-FLAG antibody (*2nd panels*). The WCE was subjected to IB with anti-Myc (*3rd panels*) or tubulin (*bottom panels*) antibody.

*Ubiquitination and Degradation of Endogenous eIF4E*—We then wished to see the ubiquitination of endogenous eIF4E (Fig. 10*A*). It was not visible under normal condition, but mono-ubiquitinated endogenous eIF4E was detected (Fig. 10*A*, *middle panel, lane 3*) when cells were heat shocked, eIF4E protein was concentrated by $m^7$GTP-Sepharose precipitation, and highly effective ECL solution was used. The 24-kDa band for endogenous eIF4E whited out (Fig. 10*A*, *middle panel*) because the ECL solution was too strong.

In Fig. 10, *B* and *C*, we carried out pulse-chase labeling of endogenous eIF4E. With heat shock, the levels of eIF4E decreased more rapidly (down to 55% at 15 h) and addition of MG132, an inhibitor of proteasome-dependent degradation pathway, restored the levels. These results indicate that endogenous eIF4E protein is also degraded in the Ub/proteasome-dependent manner.

## DISCUSSION

Protein synthesis is a tightly controlled process essential for cell survival, and in this study we described the ubiquitination and proteasome-dependent degradation of the cap-binding protein eIF4E. We summarize our working hypothesis in supplemental Fig. S2.

We identified the most probable site for Ub conjugation as Lys-159. The crystal structure of eIF4E has been solved (23–25), and Lys-159 is in the middle of two β-sheets, S5 and S6. The side chain of this residue protrudes outward (25), suggesting it is readily accessible for Ub conjugation by E3 ligases. Interestingly, there is a relationship between Lys-159 and the phosphorylated residue Ser-209. Phosphorylation of Ser-209 causes a retractable salt bridge to form with Lys-159 to clamp the cap moiety and thereby lead to increased binding of capped mRNA (23, 26). In addition, because the K159A mutant exhibited reduced association with cap analogues (27), Lys-159 is involved in the binding of capped mRNA. However, we saw no reduction in $m^7$GTP association with the K159R mutant (Fig. 3). Additionally, we did not observe reduced $m^7$GTP association with ubiquitinated eIF4E. The attachment of a Ub molecule to Lys-159 might stabilize the distance between Ser-209

Heat shock and Chip expression could additively or synergistically enhance eIF4E ubiquitination. We co-transfected cells with FLAG-tagged eIF4E, HA-Ub, and/or Myc-Chip, and samples were collected 2 h after heat shock (45 °C 10 min) (Fig. 9*C*). Although heat shock or Chip expression independently induced the ubiquitination of eIF4E (Fig. 9*C*, *top panel, lanes 3* and *4*), the combination of heat shock and Chip expression did not increase ubiquitination levels (*lane 5*). It is likely that each condition alone induced maximal eIF4E ubiquitination.

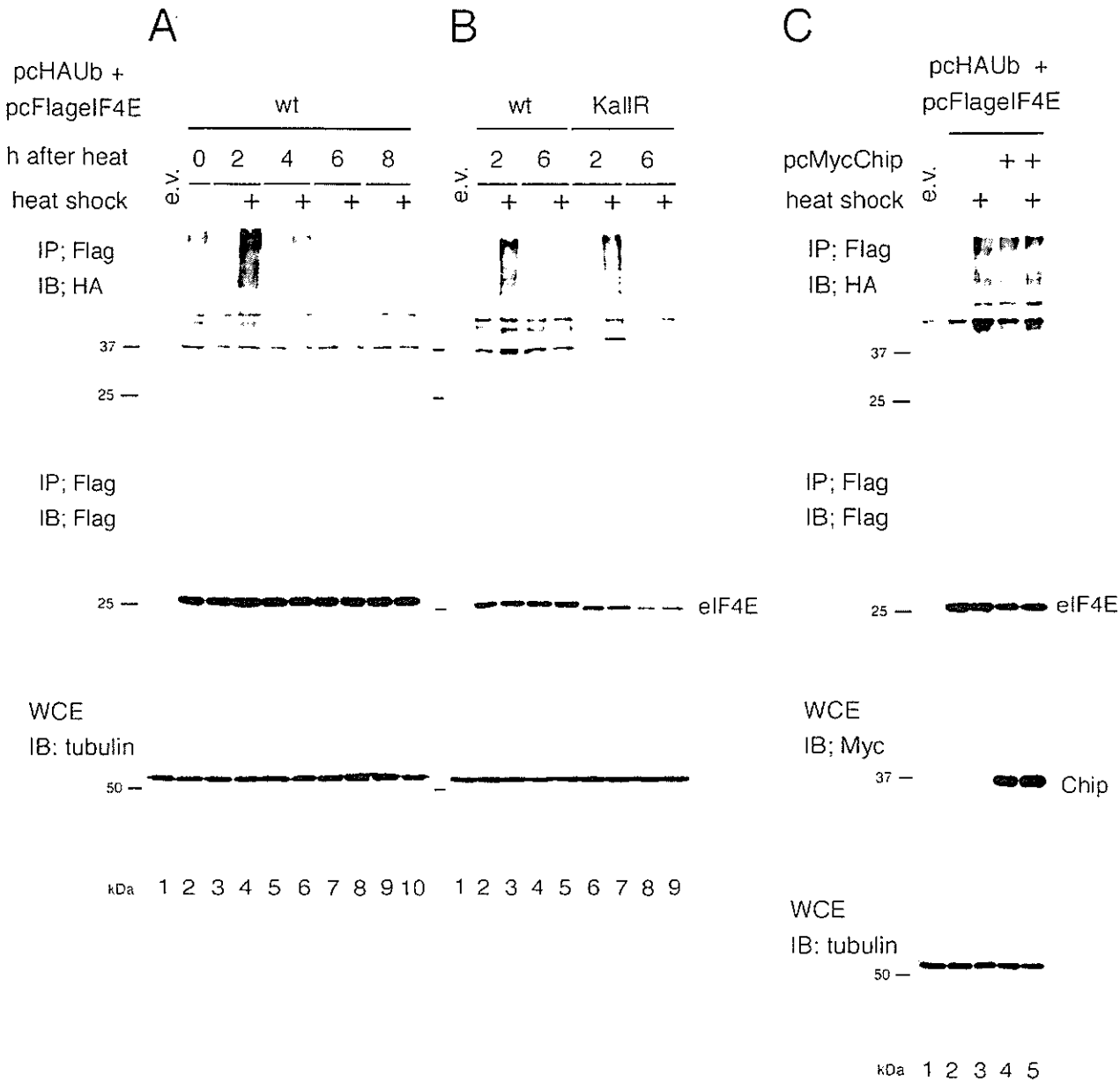


FIGURE 9. **Increased ubiquitination of eIF4E following heat shock.** *A* and *B*, heat shock enhanced eIF4E ubiquitination. Cells were transfected with pcHAUb and WT (*A*, *B*) or the KallR mutant (*B*) of pcFLAGeIF4E. 24 h after transfection, cells were heat shocked at 45 °C for 10 min (+) or not, followed by incubation at 37 °C for the indicated time. The cell lysates were subjected to IP with anti-FLAG antibody, followed by IB with anti-HA antibody (*top panels*). The membrane was then stripped and reprobed with anti-FLAG antibody (*middle*). Levels of tubulin in the WCE were also examined (*bottom*). *C*, heat shock and Chip did not additively increase eIF4E ubiquitination. Cells were transfected with pcHAUb, pcFLAGeIF4E, and/or with pcMycChip. 24 h after transfection cells were heat shocked at 45 °C for 10 min (+) or not, followed by incubation at 37 °C for 2 h. The cell lysates were subjected to IP with anti-FLAG antibody, followed by IB with anti-HA antibody (*top panel*). The membrane was then stripped and reprobed with anti-FLAG antibody (*2nd panel*). Levels of Chip (*3rd panel*) and tubulin (*bottom*) in the WCE were also assessed.

(S7-S8 loop) and Lys-159 (S5-S6 loop), similar to phosphorylation (23). Alternatively, the Ub molecule may form a bridge between Ser-209 (S7-S8 loop) and Lys-159 (S5-S6 loop) and hold the triphosphate moiety tightly. Additionally, ubiquitination of the S209A mutant of eIF4E was comparable with WT, suggesting that phosphorylation does not affect ubiquitination (Fig. 1*C*).

The W73A mutant of eIF4E, which only weakly binds eIF4G/4E-BP, showed enhanced ubiquitination and proteasome-dependent degradation (Fig. 1). What is more, expression of 4E-BP clearly reduced the levels of eIF4E ubiquitination and degradation (Fig. 6). Because the only known role for 4E-BP has been as inhibitor of cap-mediated translation initiation, we are suggesting a novel role for 4E-BP as a protector of eIF4E. 4E-BP can inhibit cap-mediated protein synthesis by binding eIF4E, but at the same time may preserve a population of inactive eIF4E-mRNA complexes by preventing eIF4E degradation. Several reports have linked 4E-BP to cellular stress (28–30). 4E-BP binds eIF4E under conditions of stress or reduced growth stimuli. When cells are removed from stress and growth conditions become favorable,

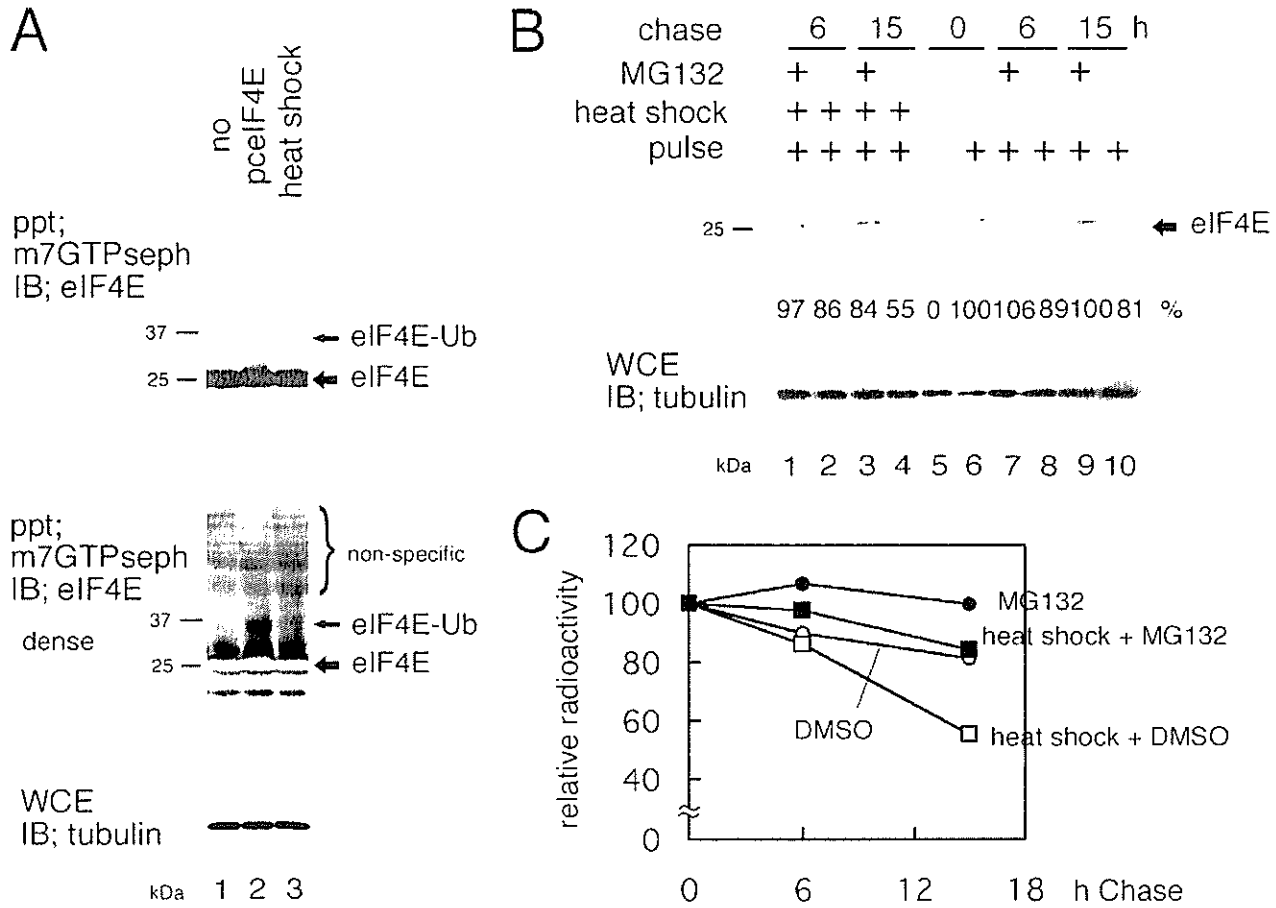


FIGURE 10. **Ubiquitination and degradation of endogenous eIF4E.** *A*, ubiquitination of endogenous eIF4E. Cells were heat shocked (*lane 3*) or mock treated (*lane 1*). As a positive control, cells were transfected with pceIF4E (*lane 2*) for 24 h. Lysates were precipitated with $m^7$GTP-Sepharose and subjected to SDS-PAGE and IB with anti-eIF4E antibody (*top* and *2nd panels*). As a control, a portion of the WCE was directly subjected to SDS-PAGE and IB was performed with anti-tubulin antibody (*bottom panel*). To assess ubiquitination levels of endogenous eIF4E, the membrane in the *top panel* was overexposed in the *2nd panel*, using highly efficient ECL solution (see "Experimental Procedures"). *B* and *C*, proteasome-dependent degradation of endogenous eIF4E. Cells were pulse labeled with [$^{35}$S]Met (36) for 3 h, washed extensively, and then incubated with cold chase medium with or without MG132 for the indicated hours. Cells for *lanes 1–4* were heat shocked immediately after the pulse label. The lysates were purified with $m^7$GTP-Sepharose and subjected to SDS-PAGE, and the radioactivity was visualized using BAS2000 system (*B, upper panel*). As a control, a portion of the WCE was directly subjected to IB with anti-tubulin antibody (*lower panel*). *C*, radioactivities in *panel B* (*upper*) were determined and shown as a line chart.

pre-existing eIF4E-mRNA complexes can be used for immediate protein synthesis after 4E-BP release. Thus, 4E-BP buffers stress by suppressing protein synthesis and preparing cells for a swift recovery.

It is quite interesting to find that the levels of endogenous eIF4E ubiquitination were very low (*e.g.* Fig. 10*A*), whereas degradation of the protein was relatively clear (*e.g.* Fig. 10, *B* and *C*). Ubiquitinated fraction was <1% in Fig. 10*A*, whereas the eIF4E decreased by 45% at 15 h after heat shock in Fig. 10, *B* and *C*. This is similar to the ubiquitination/degradation of the W73A mutant in that most of the W73A mutant protein stayed non-ubiquitinated (Fig. 1*C*, *middle panel*, *lane 6*), whereas >90% of eIF4E degraded at 48 h (Fig. 1*E*, *upper panel*, *lane 4*). We thus speculate that the efficiency of Ub conjugation is the bottleneck, and once ubiquitinated, it is proteolyzed rapidly.

The mechanism of eIF4E ubiquitination/degradation is similar to that of the endoplasmic reticulum membrane-tethered dolichol-phosphate-mannose (DPM) synthase (31). DPM1 is tethered by DPM3 to the membrane. When tethering is abolished and DPM1 becomes free, DPM1 is rapidly ubiquitinated by Chip and degraded by the proteasome. Telomeric repeat binding factor 1 and E2F transcription factors are also protected from Ub targeting and degradation by binding their partners, and these proteins are degraded after binding partner release (32, 33). Because these proteins function as complexes, it is likely important to regulate the levels of the free proteins. Thus, this may be a common mechanism of protein expression regulation in cells.

When examining the bottom panel of Fig. 6*B*, levels of 4E-BP, especially 4E-BP2 and 3, were increased by the addition of MG132. This suggests that 4E-BP is degraded in a Ub/proteasome-dependent manner. As 4E-BP is an important regulator of protein synthesis, the regulation of this process is of great interest.

During the preparation of this report, Othumpangat *et al.* (11) reported that eIF4E is proteolyzed after ubiquitination when cells are exposed to cadmium chloride. We confirmed this finding (data not shown), and because cadmium presumably acts as a cell stressor, this finding supports our hypothesis that Ub modification of eIF4E is enhanced following cell stress.